SECURITY INFORMATION

CONFIDENTIAL

Copy 184
RM L51I11

A. L. Sibila

NACA RM L51I11

c-4

NACA

RESEARCH MEMORANDUM

STUDIES OF THE USE OF FREON-12 AS A TESTING MEDIUM IN THE LANGLEY LOW-TURBULENCE PRESSURE TUNNEL

By Albert E. von Doenhoff and Albert L. Braslow

Langley Aeronautical Laboratory
Langley Field, Va.

CLASSIFICATION CHANGED TO Unclassified
BY AUTHORITY OF NASA Bull. #71
ON 1/23/62 OF JEC

CLASSIFIED DOCUMENT

This material contains information affecting the National Defense of the United States within the meaning of the espionage laws, Title 18, U.S.C., Secs. 793 and 794, the transmission or revelation of which in any manner to unauthorized person is prohibited by law.

NATIONAL ADVISORY COMMITTEE
FOR AERONAUTICS

WASHINGTON
December 5, 1951

RM L51I11

CONFIDENTIAL

NACA RM L51I11

[redacted]

NATIONAL ADVISORY COMMITTEE FOR AERONAUTICS

RESEARCH MEMORANDUM

STUDIES OF THE USE OF FREON-12 AS A TESTING MEDIUM IN THE LANGLEY LOW-TURBULENCE PRESSURE TUNNEL

By Albert E. von Doenhoff and Albert L. Braslow

SUMMARY

A number of studies relating to the use of Freon-12 as a testing medium in the Langley low-turbulence pressure tunnel have been made. With no change in the tunnel drive system, the use of Freon-12 as a testing medium increased the maximum attainable test section Mach number from approximately 0.4 to nearly 1.0 with a maximum Reynolds number of 9.5×10^6 per foot of model chord. Because of the fact that the ratio of specific heats is approximately 1.13 for Freon-12 as compared with 1.4 for air, some differences exist between data obtained in Freon-12 and in air. Methods for predicting aerodynamic characteristics of bodies in air from data obtained in Freon-12, however, have been developed from the concept of similarity of the streamline pattern. These methods, derived from consideration of two-dimensional flow, provide substantial agreement in all cases for which comparative data are available. These data consist of measurements throughout a range of Mach numbers from approximately 0.4 to 0.93 of pressure distributions and hinge moments on swept and unswept wings having aspect ratios ranging from 4.0 to 9.0 including cases where a substantial part of the wing was stalled.

INTRODUCTION

Since the publication of reference 1, equipment has been added to the Langley low-turbulence pressure tunnel to permit operation with Freon-12 (CCl_2F_2) as the testing medium. By replacing the air in the tunnel with Freon-12 at an absolute pressure of 28 inches of mercury or less, it was possible to obtain a flow Mach number of approximately 1 without any increase in the tunnel power beyond that previously available (reference 1) and without making any changes to the propeller. Under such conditions (stagnation pressure of 28 inches of mercury and Mach number of 1), the Reynolds number is approximately 9.5×10^6 per foot.

[redacted]

As indicated in references 2 and 3, Freon-12 is well adapted to use as a wind-tunnel testing medium from considerations of density, commercial availability at practical cost, chemical inertness, nontoxicity, low-vibrational heat-capacity lag, and low boiling point. Its specific-heat ratio γ, however, is only about 1.13 as compared with 1.4 for air so that significant quantitative differences exist between the compressibility relations for air and Freon. For this reason considerable uncertainty remains concerning the relation between data obtained for a model tested in Freon and data for the same model tested in air.

The studies reported in the present paper were undertaken in an effort to help resolve this uncertainty. Pressure measurements were made for two small nozzles with both air and Freon. In addition, pressure measurements with Freon in the wind tunnel were made for an unswept wing and a wing having 45° of sweepback for which corresponding data in air had previously been obtained (references 4 and 5). Hinge-moment measurements were also made in Freon for an elevator on an unswept tail surface for which corresponding data in air were available (reference 6).

As will be shown, differences were found to exist between the air and Freon data which became appreciable at transonic stream Mach numbers; however, a simple tentative method was developed based on considerations of flow geometry by means of which both Mach number and aerodynamic coefficients are subjected to slight corrections. These corrections brought the Freon and air data into substantial agreement. This method and the various tentative correction curves and procedures based on it are also described and discussed in the present paper. Subsequent data obtained in the Langley low-turbulence pressure tunnel with Freon-12 will, at least for the present, be corrected to corresponding air data by these methods although some modification may be found desirable as additional air-Freon comparison data accumulate.

SYMBOLS AND COEFFICIENTS

A	stream-tube area or aspect ratio
Λ	sweep angle of 0.25-chord line of two wing models and of 0.70-chord line of tail-surface model
λ	taper ratio, ratio of tip chord to root chord
b	span of wing

c	section chord of wing, measured parallel to plane of symmetry of model
H	total pressure
M	Mach number
p	static pressure
P	pressure coefficient $\left(\frac{p - p_o}{q_o}\right)$
q	dynamic pressure $\left(\frac{1}{2}\rho V^2\right)$
S	pressure coefficient $\left(\frac{H_o - p}{q_o}\right)$
S_R	local load coefficient $(S_U - S_L)$
V	velocity
x	distance from leading edge along section chord of wing
y	distance normal to free stream in lift direction
α	angle of attack
γ	ratio of specific heat at constant pressure to specific heat at constant volume
δ	flap deflection, degrees unless otherwise noted
ρ	mass density
c_d	wing-section wake-drag coefficient
C_{D_i}	wing induced-drag coefficient
C_D	total wing drag coefficient, wake-drag coefficient plus induced-drag coefficient
c_h	section hinge-moment coefficient for flap

[redacted]

C_h elevator hinge-moment coefficient

C_L wing lift coefficient

c_m section pitching-moment coefficient about 0.25c

c_n section normal-force coefficient

ΔC_d, ΔC_{D_i}, Δc_h, ΔC_L, Δc_m, Δc_n, ΔS_R } coefficient in Freon-12 minus corresponding coefficient in air

Subscripts:

A air

F Freon-12

U upper surface

L lower surface

o conditions in free stream

1 conditions in wake

2 conditions at orifice 2 for nozzle tests

cr conditions at a local Mach number of 1.0

COMPARISON OF NOZZLE FLOWS

Nozzle tests.- In order to obtain comparative data for some simple two-dimensional flows, pressure-distribution measurements of the flow

[redacted]

about two bumps in a 1-inch nozzle were made in both Freon-12 and air. Sketches of the nozzle arrangement and bumps are presented in figures 1 and 2. One of the bumps was rather long and thick. In this case the opposite wall of the nozzle was curved to provide a reasonable margin between the lowest Mach number at which the speed of sound occurred locally and the nozzle choking condition. The second configuration consisted of a small bump with the opposite wall of the nozzle straight. In each case the gas was forced through the nozzle from large-capacity high-pressure storage tanks. For the Freon tests, in order to avoid conditions close to condensation, the gas was heated before passing through the nozzle into a large evacuated chamber.

The nozzles were cast from bismuth-tin alloy and the surfaces were polished. Pressure tubes were cast into the nozzle and were located as shown in figures 1 and 2. Rubber gaskets, cut to fit the nozzle contours, served to seal the nozzle blocks to glass side walls of the section. Manometer readings were recorded by means of cameras.

The two bumps in the 1-inch wide nozzle were tested in Freon-12 through a range of Mach number from just below the critical speed to nozzle choke and then retested in air through a similar range of Mach number. The Reynolds numbers for the air tests were maintained approximately the same as for the Freon tests by adjusting the stagnation pressures to the required values. The values of the absolute stagnation pressure during the Freon and air tests were approximately 29 and 76 inches of mercury, respectively. The nozzles were not altered in any way between the Freon and air tests.

The Mach number at static orifice 2 is used as the reference Mach number. If the bump in the nozzle is considered to be crudely representative of an airfoil mounted in a two-dimensional tunnel, the values of local Mach number at orifice 2 M_2 are not free-stream values because of the close proximity of orifice 2 to the bump (fig. 2) but correspond to free-stream Mach numbers that are somewhat higher.

Comparison of results; streamline similarity concept.- The pressure coefficient S obtained in air and in Freon-12 at each orifice location is plotted against M_2 in figures 3 and 4. These data do not indicate any large differences in results obtained in Freon-12 as compared to those obtained in air except near the maximum Mach number attainable. There is some indication that the choke Mach number in Freon-12 is slightly greater than in air.

The differences between Freon and air results shown in figures 3 and 4 led to more detailed consideration of the relationship between flows in Freon and in air and to the present proposal that a correspondence between the flows might be based more accurately on the concept of geometrical similarity of the streamline pattern. If such streamline

[redacted]

similarity exists, then the ratio of the stream-tube areas at any two positions for Freon flow must be equal to the ratio of the stream-tube areas at the same positions for air flow. Furthermore, in either gas the stream-tube area is a minimum when the speed of flow is equal to the local speed of sound. The range of physically possible streamline spacings in either gas may then be represented by values of the ratio A_{cr}/A ranging from 1.0 to 0.

The variable A_{cr}/A may be considered a flow parameter in the same sense as the Mach number. The relationship between A_{cr}/A and the Mach number for air and Freon is given in figure 5. It is seen from figure 5 that the variation of A_{cr}/A with Mach number is very nearly the same for air and Freon-12 up to a Mach number of about 1.4. The differences in A_{cr}/A increase progressively with increasing Mach number above a value of 1.0.

In order that the same range of streamline spacings be available in both gases, as is necessary if streamline similarity is to be generally possible, it is necessary that the relative streamline spacing be expressed in terms of the variable A_{cr}/A, where A_{cr} is the streamline spacing corresponding to a local Mach number of 1.0. If the area at some Mach number other than unity were chosen as the reference area - for example, the area at 0.8 Mach number, $A_{0.8}$ - then there would be a range of Mach numbers near unity for which values of $A_{0.8}/A$ for Freon would exceed the highest possible value of $A_{0.8}/A$ for air.

Streamline similarity and the transonic similarity rule.- An indication of the possibility of the existence of streamline similarity is afforded by a study of the rule for transonic similarity given in reference 7. According to the transonic similarity law developed for flows in which the local Mach numbers throughout the field are nearly equal to 1.0, if the following substitution of variables is made

$$\xi = \frac{x}{a}$$

$$\eta = \frac{y}{a}\left[(\gamma + 1)t\right]^{1/3}$$

$$f(\xi,\eta) = \frac{\phi}{ac^*}$$

where

x, y rectangular coordinates in physical plane

a half chord of body

t maximum thickness ratio of body

ϕ velocity potential in physical plane

c^* velocity of sound at local Mach number of 1.0

ξ nondimensional coordinate in stream direction

η nondimensional coordinate perpendicular to stream direction

$f(\xi,\eta)$ nondimensional velocity potential

the differential equation of motion becomes

$$\frac{\partial^2 f}{\partial \eta^2} = 2K \frac{\partial f}{\partial \xi} \frac{\partial^2 f}{\partial \xi^2}$$

where

$$K = (1 - M_\infty)\left[(\gamma + 1)t\right]^{-2/3}$$

and

M_∞ free-stream Mach number

To obtain similar flows in the sense of reference 7, K must remain constant as M_∞, γ, and t are varied. In order to show that a corresponding relation must hold throughout the field of flow, let

$$K_l = (1 - M)\left[(\gamma + 1)t\right]^{-2/3}$$

be a quantity analagous to the transonic similarity parameter K but formed with the local Mach number M rather than the free-stream Mach number M_∞. It is shown in reference 8, that

$$K_l = -K^{-2/3} \frac{\partial f}{\partial \xi}$$

Since, for similar solutions, $\partial f/\partial \xi$ at a given point ξ,η in the field of flow is independent of variations of M_∞, γ, and t, the value of K_l formed for any point ξ,η in the field must also remain constant.

[redacted]

Since K_l is a function of three variables, M, γ, and t at any point ξ,η in the field, it is permissible to assume an arbitrary definite relationship between two of the variables and adjust the third so as to maintain similarity. With this idea in mind, let $t = \frac{C_1}{(\gamma + 1)^{1/4}}$ where C_1 is an arbitrary constant. Then, $(1 - M)\left[C_1(\gamma + 1)^{3/4}\right]^{-2/3}$ or $(1 - M)\left[C_1^{-2/3}(\gamma + 1)^{-1/2}\right]$ must be a constant, that is, $(1 - M)$ must vary directly as $(\gamma + 1)^{1/2}$.

Consider the relationship between M and γ required for streamline similarity. The equation relating the area ratio, Mach number, and γ is as follows:

$$\frac{A}{A_{cr}} = \frac{\left[1 + \frac{\gamma - 1}{2}(1 - M^*)^2\right]^{\frac{\gamma+1}{2(\gamma-1)}}}{1 - M^*}\left(\frac{2}{\gamma + 1}\right)^{\frac{\gamma+1}{2(\gamma-1)}}$$

where M^* is $1 - M$. If this expression is expanded in powers of M^* and terms containing powers of M^* greater than 2 are neglected then

$$\frac{A}{A_{cr}} = \frac{2}{\gamma + 1} M^{*2} + 1$$

As indicated previously, if streamline similarity is to be obtained, the value of A/A_{cr} at corresponding points in the field must remain unchanged as γ is varied. In accordance with this condition, then, $M^{*2} = C_2(\gamma + 1)$, where the value of C_2 depends on the value of A/A_{cr} at the particular point in question or $1 - M$ varies directly as $(\gamma + 1)^{1/2}$. It is thus seen that streamline similarity is consistent with a special case of the general transonic similarity rule. Strictly speaking, then, streamline similarity to the accuracy of the transonic similarity rule would be obtained in two-dimensional flows in air and Freon-12 if the body tested

in Freon were $\left(\frac{1 + 1.4}{1 + 1.128}\right)^{1/4}$ or 1.030 times as thick as the body tested in air and the free-stream Mach number in Freon were $1 - \left(\frac{1 + 1.128}{1 + 1.4}\right)^{1/2}(1 - M_A)$ or $0.943M_A + 0.057$. Because of the small magnitude of the correction to the thickness ratio, it is thought that no appreciable error will result if the model tested in Freon has the same thickness ratio as that for which data are desired in air.

A further indication of the existence of streamline similarity is afforded by a study of the comparative pressure-distribution data presented in figures 3 and 4. At any particular stream speed as indicated by the value of M_2 in Freon, the distribution of values of A_{cr}/A in Freon can be computed from the basic pressure-distribution data by application of the relations for isentropic gas flow. If streamline similarity is assumed, the values of A_{cr}/A for air flow will be the same at corresponding points. By reversing the preceding process but by using the value of γ appropriate to air, the corresponding values of local pressure coefficient can be computed for air. If these computed values of the pressure coefficients for air agree with those measured in air, the agreement will be an indication that streamline similarity exists. The aforementioned procedure has been carried out in the preparation of figures 6 and 7; that is, the Freon data have been converted to equivalent air data. It is to be noted that, in the process of converting from Freon to air through the area-ratio concept, slight changes in local Mach numbers as indicated in figure 5 are necessary. Hence, for example, a local Mach number of 0.80 in Freon is equivalent to a local Mach number of 0.786 in air.

The converted Freon data in figures 6 and 7 are in much closer agreement with the actual air data than the corresponding data of figures 3 and 4. In fact the converted Freon data and the air data agree almost within the limits of experimental accuracy.

Another comparison between the flows in Freon and in air is given in figures 8 and 9 in which the distribution of local Mach number over the surface of the bumps is given for several reference Mach numbers M_2. In these figures the Freon data have been converted to equivalent air data by means of the assumption of streamline similarity; that is, local values of A_{cr}/A would be the same in the two gases. In figures 8 and 9 agreement of local values of M as between air and Freon, therefore, means that local values of A_{cr}/A are in agreement. Corresponding runs in air and in Freon compared on the basis of very nearly the same values of converted M_2, that is, A_{cr}/A at station 2, exhibited the same distribution of converted M, that is, A_{cr}/A, over the rest of the surface.

[redacted]

The fact that, almost within the limits of experimental accuracy, the distribution of A_{cr}/A ahead of and behind the shock is the same when the value of A_{cr}/A at orifice 2 is the same, indicates that, for corresponding values of A_{cr}/A, the position of the shock is the same and that there is no measurable difference in the effect of the shock on the flow.

COMPARISON OF WIND-TUNNEL PRESSURE-DISTRIBUTION DATA

The study described in the preceding section, "Comparison of Nozzle Flows" indicated that the assumption of streamline similarity for corresponding flows in air and Freon-12 was a good working hypothesis. It was realized, however, that similarity of flows over a bump in a nozzle is not necessarily a general indication that such flow similarity in air and Freon-12 would exist over such bodies as airfoils and wings, because of the absence of conditions required to determine the circulation and the virtual absence of flow separation in the presence of shocks. In order to obtain more representative data to investigate the correspondence of flows in air and Freon-12 more completely, measurements were made in Freon-12 in the Langley low-turbulence pressure tunnel of the distribution of pressure over a high-aspect-ratio unswept wing and a sweptback-wing-fuselage model, both of which had been originally tested in the Langley 8-foot high-speed tunnel (references 4 and 5).

The unswept wing model was a full-span wing of aspect ratio 9 and taper ratio 0.4, with NACA 65-210 airfoil sections. Static-pressure orifices were located on the upper and lower surfaces at eight spanwise stations: 11-, 20-, 30-, and 43-percent semispan on the left half of the wing and 56-, 64-, 80-, and 95-percent semispan on the right half of the wing. The model was equipped with a 20-percent-chord plain aileron which was undeflected for these tests. A more complete description of the model is presented in reference 4.

The sweptback wing-fuselage model was a full-span midwing configuration. The wing had the 0.25-chord line swept back 45°, an aspect ratio of 4, a taper ratio of 0.6, and NACA 65A006 airfoils in the stream direction. The fuselage was made by cutting off the rear part of a body of revolution of fineness ratio 12 to form one with a fineness ratio of 10. Static-pressure orifices were located on both wing surfaces at five spanwise stations: 20-, 60-, and 95-percent semispan on the left half of the wing and 40- and 80-percent semispan on the right half of the wing. Ordinates of the fuselage and other dimensional details are presented in reference 5.

Each model was tested in the low-turbulence pressure tunnel as a semispan model mounted off one tunnel wall; whereas each had previously been

[redacted]

tested in a full-span arrangement in the Langley 8-foot high-speed tunnel. In the 8-foot high-speed tunnel the unswept wing was mounted on a vertical plate in the center of the tunnel and the swept-wing model was mounted on a sting-supported fuselage. The semispan swept-wing model as tested in the low-turbulence pressure tunnel included a half fuselage. The area of the 8-foot-tunnel test section is about twice that of the low-turbulence pressure tunnel so that the tunnel blocking effects for the tests in the two tunnels were approximately the same.

The models were tested in Freon-12 at the same Reynolds number and through the same range of Mach number and angle of attack used in the original tests in air. The aileron deflection on the unswept wing model, which was inadvertently set at -0.3° rather than an intended 0° for the tests of reference 4, was maintained the same for the tests in Freon-12. The tests consisted of measurements of the pressure distribution at all 8 spanwise stations on the unswept wing and the pressure distribution at 3 of the 5 spanwise stations on the swept wing (20-, 60-, and 95-percent semispan).

Representative comparisons of the chordwise distribution of pressure over the unswept wing in air and in Freon-12 are presented in figure 10. These data were obtained at an angle of attack of 4° at a station 30 percent of the semispan from the root. Although the data of figure 10 are only a small part of the large amount of comparative data obtained for this model, they are representative of the large changes in shape of pressure distribution that occur between subcritical and supercritical Mach numbers and correspond to the highest angle of attack for which published pressure-distribution data are available at Mach numbers greater than 0.9 (reference 4). The conclusions indicated by an examination of figure 10 are the same as would be obtained from an examination of the remaining mass of comparative data. In this figure the pressure coefficient P is plotted against the percent chord for Mach numbers of 0.400, 0.850, 0.900, and 0.924. The Freon pressure coefficients and free-stream Mach numbers have been converted to corresponding air data by means of the assumption of streamline similarity.

A typical example showing the magnitude of the conversion from Freon to air conditions is given in figure 11 which corresponds to the data given for an air Mach number of 0.850 in figure 10. In figure 11, as in the case of the nozzle tests, the converted Freon data are in substantially closer agreement with the corresponding air data than the Freon data reduced in the normal fashion without conversion.

It seems apparent from figure 10 that no noticeable differences in flow phenomena exist between the air and Freon flow. The rather large changes in the shape of the pressure distribution with relatively small changes in Mach number are duplicated in the Freon flow. The shocks seem to occur at the same chordwise positions, and the pressure distributions

for the upper and lower surfaces at a Mach number of 0.9 cross at the same position. The small discrepancies between the Freon and air data noticeable for some of the test conditions can easily be accounted for on the basis of the probable errors in determining free-stream Mach number, measurement of the local pressures, angle of attack, and so forth.

Representative comparisons of the chordwise distribution of pressure over the 45° sweptback wing in air and in Freon-12 are presented in figure 12. The data presented are for stations 20- and 95-percent semispan from the model plane of symmetry and were obtained at an angle of attack of 14° at Mach numbers of 0.60 and 0.80. The Freon pressure coefficients and free-stream Mach numbers have been converted to corresponding air data by application of the streamline similarity concept to the flow in the free-stream direction. On the sweptback wing as on the straight wing, no noticeable differences in flow phenomena exist between the air and Freon flow. Application of the streamline similarity concept to the flow in the free-stream direction appears to be adequate for practical purposes, at least for aspect ratios of this order. Obviously, for an infinitely long swept wing, consistency should require that the component normal to the leading edge should be used.

The wide variety of flow conditions for which application of the streamline similarity concept led to substantial agreement of air and Freon data is to be noted. The conditions investigated include not only transonic flows at moderate angles of attack but also cases of transonic flows with strong shocks in which a large part of the wing area is stalled.

CONVERSION FACTORS FOR FORCES AND MOMENTS

The previous analysis indicated that the flow phenomena about a body in air could be predicted from measurements made about the same body in Freon-12. More particularly, the analysis indicated that the pressure distribution over a body in one medium could be predicted from the measured pressure distribution in the other medium. Since, however, wind-tunnel measurements frequently consist of the measurement of the over-all forces and moments acting on a body rather than of detailed pressure distributions, some means of interpreting force and moment measurements in Freon-12 in terms of corresponding air data is required.

In order to determine the principal factors affecting the correlation of force and moment measurements, a large quantity of wind-tunnel pressure-distribution data measured in air was converted to equivalent Freon data by means of the streamline similarity concept and the differences between the air and Freon data were studied. It is necessary that a method of force correlation produce results within the accuracy of

experimental data through a large range of Mach number, angle of attack, and body shape in order to be useful for projected test programs. For this reason and the fact that the principal aerodynamic forces for an airplane occur on a wing, pressure-distribution data obtained in the Langley 8-foot high-speed tunnel on the NACA 65-210 airfoil and in the Langley rectangular high-speed tunnel on the NACA 65,3-019 airfoil were used for this analysis. The tests on the NACA 65-210 airfoil, as reported in reference 4, covered a range of Mach number from 0.4 through 0.925 and the tests on the NACA 65,3-019 airfoil, as reported in reference 9, covered a range of Mach number from 0.43 through 0.74. The local Mach numbers in these tests were usually less than 1.50. Both airfoils were tested through a range of angle of attack from 0° to 10°. Additional data on the effect of flap deflection on the pressure distribution were available on the NACA 65,3-019 airfoil.

Normal Force, Pitching Moments, and Hinge Moments

The pressure distributions taken from the selected test data were converted from air to corresponding pressure distributions in Freon-12 by use of the assumption that the area ratio A_{cr}/A at each point in the field of flow is the same in both mediums. For each test condition, the incremental change in the pressure coefficient between air and Freon-12 was calculated at a series of points along the chord for both the upper and lower surfaces of the airfoils. The upper- and lower-surface increments at equal percents of the chord were then added to obtain the load-coefficient increment.

Representative pressure distributions in air and the corresponding distributions of load-coefficient increments between air and Freon-12 for large variations of free-stream Mach number, angle of attack, and flap deflection are shown in figures 13 and 14. The area and moment integrals of the load-coefficient increment distributions were used to obtain values of $\Delta c_n/c_{n_F}$, $\Delta c_m/c_{m_F}$, and $\Delta c_h/c_{h_F}$ which were found to be appreciably more dependent upon the free-stream Mach number than upon the magnitudes of the pressures or the shape of the pressure distribution, which varied quite radically with airfoil shape, angle of attack, flap deflection, Mach number, and presence of shock. In the angle-of-attack range where the normal-force coefficient is of the same order of magnitude as the lift coefficient, the relative magnitude of the correction to the lift coefficient can be taken the same as the correction to the normal-force coefficient.

The results of this study of a diversity of airfoil pressure distributions in air are shown in figure 15 where the force and moment increment percentages are plotted against the free-stream Mach number in Freon-12. The increment percentages were found to increase with

increasing Mach number reaching a value of $\Delta c_n/c_{n_F}$ equal to 0.075 and $\Delta c_m/c_{m_F}$ equal to 0.090 at a Mach number of 0.9.

The same procedure that was used on the airfoil pressure distributions was also used on the pressure distribution over the flap of the NACA 65,3-019 airfoil to determine the Freon-to-air correlation for hinge moments. As can be seen in figure 15, the precentage increments of c_h is a function mainly of free-stream Mach number and correlated closely with the airfoil pitching moments. The calculated points farthest from the faired curves in figure 15 usually occurred for such small values of c_n, c_m, and c_h that the error involved in using the percentage increment from the faired curve rather than the actual calculated value is negligible.

In view of the fact that the changes in pressure coefficient depend in a rather complicated way on local flow conditions, it, at first sight, seems surprising that the magnitude of the conversion factor for normal force, pitching moment, and hinge moment is nearly the same and also that it depends almost entirely on free-stream conditions and is relatively independent of lift coefficient and the shape of the particular body. An explanation of this effect is found from a detailed consideration of the variation of the correction to the local load coefficient with the magnitude of the local load coefficient. Figure 16 is a plot of the variation in difference in local load coefficient between Freon and air with the magnitude of the local load coefficient in Freon for a Freon free-stream Mach number of 0.8. It must be realized that the local load coefficient itself is the difference between the upper- and lower-surface pressure coefficients at a given position. The load coefficient can be varied in two ways. The upper-surface pressure coefficient may be held constant and the local load coefficient increased by decreasing the lower-surface pressure coefficient. Curves corresponding to this method of varying the local load coefficient are shown by the solid lines in figure 16. Conversely, the local load coefficient can be increased by holding the lower-surface pressure coefficient constant and increasing the value of the upper-surface pressure coefficient. Curves corresponding to this method of varying the local load coefficient are shown by the short-dashed lines in figure 16.

The fact that both the pitching moment and normal force have substantially the same conversion factor (fig. 15) suggests very strongly that each of the local load coefficients along the chord of the airfoil is changed by substantially the same factor. If this were so, the slope of the curve of change in local load coefficient against load coefficient would be constant at a value equal to the conversion factor given in figure 15. This line is shown as the long-dashed line (fig. 16).

It is seen in figure 16 that for low values of the upper-surface pressure (high value of the corresponding pressure coefficient) the

[redacted]

general trend of the curve of change in load coefficient against load coefficient is fairly well approximated by the long-dashed line representing the conversion factor of figure 15. Furthermore, regardless of the value of the pressure coefficient, no correction is indicated when the load coefficient is zero. The combinations of pressure coefficient and load coefficient corresponding to corrections at largest variance with that indicated by the long-dashed line are combinations of a relatively low upper-surface pressure coefficient and a large load coefficient. As a matter of general observation, the likelihood of the occurrence of large values of the load coefficient for small values of the upper-surface pressure coefficient is very small. For example, if the upper-surface pressure coefficient is small the corresponding value of the actual pressure is relatively high. Consequently, in order to have a high load coefficient the lower-surface pressure must be very close to the stagnation pressure. Except for conditions in the immediate vicinity of the leading edge, if the lower-surface pressure is near stagnation the corresponding upper-surface pressure is generally quite low, or, in other words, the upper-surface pressure coefficient is quite high. In spite of the fact, therefore, that substantial departures from the general trend are theoretically possible, for the combinations of local pressure coefficient and load coefficient likely to occur in practice the variation of the difference in local load coefficient with load coefficient is nearly linear.

Drag

In order to derive an over-all conversion factor to obtain air data from corresponding Freon drag-force-test data, it is desirable to consider the drag as being made up of two parts; the induced drag and the drag indicated by a wake survey.

Induced drag.- The induced drag for a wing in compressible flow is given by the relation $C_{D_i} = \frac{1}{\pi A}(1 + \delta)C_L{}^2$ (reference 10). The correction factor δ in this expression is a function of the wing geometry and $\sqrt{1 - M^2}\,\frac{A}{a_o}$ where M is the free-stream Mach number, A the aspect ratio of the wing, and a_o the lift-curve slope of the airfoil sections at zero Mach number. Since the differences in Mach number between corresponding flows in Freon and in air are relatively small, the value of $\frac{1 + \delta}{\pi A}$ can be taken to be the same in air and Freon at corresponding conditions. The ratio of the induced drag in air to that in Freon, therefore, may be written as

$$\frac{\left(C_{D_i}\right)_A}{\left(C_{D_i}\right)_{[redacted]}} = \frac{\left(C_L{}^2\right)_A}{\left(C_L{}^2\right)_{[redacted]}}$$

[redacted]

To the first order, then, the percentage increment in induced drag in converting from Freon to air is equal to twice the percentage increment in lift coefficient or

$$\frac{\Delta C_{D_i}}{(C_{D_i})_F} = 2\left[\frac{\Delta C_L}{(C_L)_F}\right]$$

The quantity $\Delta C_L/(C_L)_F$ is given, as stated previously, in figure 15.

Wake drag.- The wake drag of a body may be associated with flow conditions at a point sufficiently far downstream so that the static pressure has returned to the free-stream value. The method of converting Freon-to-air wake-drag measurements resulted from the assumption that the streamline similarity indicated by the nozzle pressure distributions extended to the region of the wake. The expression for the drag coefficient in terms of quantities that can be measured in the wake is

$$c_d = \frac{2}{c}\int_{\text{wake}} \left(\frac{H_1}{H_o}\right)^{\frac{\gamma-1}{\gamma}} \left[\frac{1-\left(\frac{p_o}{H_1}\right)^{\frac{\gamma-1}{\gamma}}}{1-\left(\frac{p_o}{H_o}\right)^{\frac{\gamma-1}{\gamma}}}\right]^{1/2} \left\{1-\left[\frac{1-\left(\frac{p_o}{H_1}\right)^{\frac{\gamma-1}{\gamma}}}{1-\left(\frac{p_o}{H_o}\right)^{\frac{\gamma-1}{\gamma}}}\right]^{1/2}\right\} dy_1$$

if the static pressure in the wake is taken as free-stream static pressure (reference 11). The integrand in this expression is, of course, $d(c_d/2)/d(y/c)$.

From the assumption of the same stream-tube area ratio A_{cr}/A in air and Freon both for free-stream conditions and for local conditions in the wake, values of the elemental wake-drag conversion factor

$$\frac{\left(\frac{dc_d}{dy/c}\right)_F - \left(\frac{dc_d}{dy/c}\right)_A}{\left(\frac{dc_d}{dy/c}\right)_F}$$

[redacted]

were computed as a function of $\left(\frac{H_o - H_1}{H_1 - P_o}\right)_A$ for various free-stream air Mach numbers (fig. 17). It is to be noted that for any given free-stream Mach number, the conversion factors for the various points in the wake having different total pressure losses will be along a line in figure 17 for that particular value of the free-stream Mach number. Because the value of the conversion factor varies much more with the value of the free-stream Mach number than with the loss of total pressure in the wake, it is reasonable to expect that the conversion factor for drag measured in Freon will be primarily a function of the free-stream Freon Mach number and virtually independent of the magnitude of the wake-drag coefficient. By applying the detailed wake-drag conversion factors given in figure 17 to a large variety of air wake-survey data, this condition was actually found to be the case. The over-all wake-drag conversion factor is plotted against free-stream Freon Mach number in figure 18.

Although the assumption that the stream-tube area ratios are the same for Freon and air may not be as valid when applied to the wake as when applied to the flow over the airfoil profile, the increment in wake drag was shown to reach a value of only 5.2 percent at a free-stream Mach number of 0.9. Inasmuch as this increment is relatively small, it appears that any inadequacies in the basic assumption would result in insignificant differences in the conversion from Freon to air.

Total wing drag.- The Freon-air conversion to the total wing drag coefficient requires that an estimate be made of the relative magnitudes of the wake drag and induced drag. For the purposes of determining the conversion for the total drag, the induced drag can be calculated theoretically. The remainder of the drag as measured on a balance is assumed to be wake drag. This separation of the drag into two components enables the determination of the magnitude of the over-all conversion factor. Any error in the estimate of the relative magnitude of wake and induced drag would result only in a corresponding error in the magnitude of the conversion factor which in itself is small.

The percentage increments which have been derived for the wake drag and induced drag individually can be combined to convert a total wing-drag coefficient as measured on a balance with the following equation:

$$C_{D_A} = KC_{D_F} + (K' - K)C_{D_{i_F}}$$

[redacted]

where

$$K = 1 - \frac{\Delta c_d}{c_{d_F}}$$

$$K' = 1 - 2\frac{\Delta C_L}{C_{L_F}}$$

Rolling Moment, Yawing Moment, and Side Force

The moment of a wing about a longitudinal axis is a function only of the normal force acting on the wing. The conversion of rolling-moment coefficients measured in Freon-12 to corresponding coefficients in air, therefore, is considered to be the same as the conversion for the normal-force coefficient.

The magnitude of the conversion factors for yawing moment and side force depends upon the nature and origin of the forces involved and so may vary with different configurations under investigation. For example, the yawing moment contributed by a deflected spoiler is caused by an increase in wake drag; whereas the yawing moment contributed by a downwardly deflected aileron may be caused predominantly by an increase in induced drag. The conversion for yawing moment and side force, therefore, should be determined for each individual configuration after consideration of the forces involved.

Application to Swept Wings

The application of the streamline-similarity criterion to the flow over swept wings is not quite as apparent as the application to the flow over unswept wings. It is not obvious whether the area-ratio criterion should be applied to the simple sweep theory, that is, to the flow normal to the wing leading edge, or whether it should be applied to the flow in the stream direction. An inconsistency in results exists between the simple sweep theory and a rigid application of the area-ratio concept. Inasmuch as the actual flow over a swept wing of reasonably low aspect ratio is a combination of the two types of flow, for simplicity in applying the conversion from Freon to air, application of the area-ratio concept to the flow in the free-stream direction will be used. As indicated in a previous section from comparison of experimental data obtained in Freon and in air on a swept wing, the application of the area-ratio concept to the flow in the free-stream direction appeared to be adequate for practical purposes.

[redacted]

In order to obtain an indication of the magnitude of the differences involved in the application of the streamline-similarity concept to the stream flow rather than the flow normal to the wing leading edge, consider the flow about a wing swept back 45° at a Freon free-stream Mach number of 0.9. Application of the streamline-similarity concept to the stream direction and to the normal flow indicates that the values of free-stream Mach number in air are 0.894 and 0.884, respectively. Although this difference in Mach number increases with sweep angle, the importance of an error in the actual free-stream Mach number decreases with sweep inasmuch as the effect of changes in Mach number on the aerodynamic characteristics in the subsonic range is appreciably reduced as the sweep is increased. The conversion factor for the normal-force coefficient for the 45° swept wing at a Freon free-stream Mach number of 0.9 is 7.3 percent when based on the stream flow and 5.0 percent when based on the normal flow. Inasmuch as the flow over a swept wing of relatively low aspect ratio is a combination of the two types of flow, as mentioned previously, the correct value of the conversion factor for such a wing is probably between the two extremes indicated.

COMPARISON OF HINGE-MOMENT DATA

Inasmuch as any possible differences between Freon and air-flow conditions might be expected to be of the largest magnitude near the trailing edge of a body, it was thought that a critical check of Freon data could be obtained by a comparison of the hinge moments of a trailing-edge control surface measured in Freon and in air. Furthermore, such a comparison would also serve as a check on the method of converting moments described in the preceding section. The tail-surface model used for this comparison was a full-span unswept wing of aspect ratio 4.01 and taper ratio 0.5 with NACA 65-108 airfoil sections and was equipped with a 0.30-chord sealed, unbalanced elevator. More detailed information on this model is presented in reference 6.

A comparison with air data of the hinge-moment measurements made on the tail-surface model in Freon are presented in figure 19 for a range of Mach numbers from 0.775 to 0.907 for various angles of attack and control-surface deflection. An indication of the degree of accuracy of the data is presented in figure 20 where the hinge-moment data obtained in air in both the Langley 8-foot high-speed tunnel and in the Langley low-turbulence pressure tunnel at a Mach number of 0.400 are compared. It is apparent in figure 19 that the agreement of the Freon and air hinge-moment data is substantially as close as the corresponding comparative measurements made only in air (fig. 20). Thus, in every case in which comparative data in Freon-12 and in air are available excellent agreement has been obtained.

[redacted]

MODIFICATIONS TO THE LANGLEY LOW-TURBULENCE PRESSURE TUNNEL FOR THE USE OF FREON-12

Several modifications have been made to the Langley low-turbulence pressure tunnel since a description of it was published in reference 1. It may be of interest here to mention some of these changes and to describe the characteristics of the modified tunnel.

For obvious reasons, it is necessary to be able to store the Freon removed from the tunnel and to separate Freon from an air-Freon mixture. To accomplish this end, equipment having a capacity of 600 cubic feet per minute at atmospheric pressure was provided which removes the gas from the tunnel and compresses and cools it in stages to an ultimate pressure of 1800 pounds per square inch and a temperature of -50° F. Under these conditions nearly all of the Freon has been condensed and the high-pressure gas discharged to atmosphere is nearly all air.

The primary physical change to the tunnel air passage has been the installation of a new test section to permit testing in Freon-12 at high subsonic Mach numbers. The original section had constrictions upstream and downstream of the test region which had to be removed for tests at high Mach numbers. The new test section is the same size as the original but the side walls are expanded to allow for the growth of the wall boundary layer. The longitudinal distribution of Mach number along the tunnel center line is presented in figure 21. Each curve, of course, is for a different propeller rotational speed. The data indicate that the side walls are expanded sufficiently to obtain a uniform distribution of Mach number through the test section up to a Mach number of about 0.97. The original drive motor and propeller are being used and with these it is possible to choke the tunnel as evidenced by the region of supersonic flow at the highest test Mach number in figure 21.

When Freon-12 is used as a testing medium the Mach number and Reynolds number can be varied independently simply by changing the stagnation pressure of the Freon. The Mach number can be increased to tunnel choke for a range of absolute stagnation pressure from approximately 6 to 28 inches of mercury and the range of Reynolds number that can be covered at each Mach number is correspondingly large. For example, at a Mach number of over 0.9, the Reynolds number range is from approximately 2.5×10^6 to 9.5×10^6 per foot of chord.

A 60-mesh screen and two of the original 11 turbulence-reducing 30-mesh screens (reference 1) have been removed. In addition, boundary-layer suction slots in the test section side walls have been removed. These alterations have increased the energy ratio of the tunnel somewhat but have not caused any noticeable increase in the low-turbulence level

[redacted]

as evidenced by measurements of the critical boundary-layer Reynolds number on the same airfoil model in both test sections; at the same chordwise position, the same critical boundary-layer Reynolds number was measured in both test sections.

CONCLUDING REMARKS

A number of studies relating to the use of Freon-12 as a testing medium in the Langley low-turbulence pressure tunnel have been made. With no change in the tunnel drive system, the use of Freon-12 as a testing medium increased the maximum attainable test section Mach number from approximately 0.4 to nearly 1.0 with a maximum Reynolds number of 9.5×10^6 per foot of model chord. Because of the fact that the ratio of specific heats is approximately 1.13 for Freon-12 as compared with 1.4 for air, some differences exist between data obtained in Freon-12 and in air. Methods for predicting aerodynamic characteristics of bodies in air from data obtained in Freon-12, however, have been developed from the concept of similarity of the streamline pattern. These methods, derived from consideration of two-dimensional flows, provide substantial agreement in all cases for which comparative data are available. These data consist of measurements throughout a range of Mach number from approximately 0.4 to 0.93 of pressure distributions and hinge moments on swept and unswept wings having aspect ratios ranging from 4.0 to 9.0 including cases where a substantial part of the wing was stalled.

Langley Aeronautical Laboratory
National Advisory Committee for Aeronautics
Langley Field, Va.

[redacted]

REFERENCES

1. Von Doenhoff, Albert E., and Abbott, Frank T., Jr.: The Langley Two-Dimensional Low-Turbulence Pressure Tunnel. NACA TN 1283, 1947.

2. Smelt, R.: Power Economy in High-Speed Wind Tunnels by Choice of Working Fluid and Temperature. Rep. No. Aero. 2081, British R.A.E., Aug. 1945.

3. Huber, Paul W.: Use of Freon-12 as a Fluid for Aerodynamic Testing. NACA TN 1024, 1946.

4. Whitcomb, Richard T.: Investigation of the Characteristics of a High-Aspect-Ratio Wing in the Langley 8-Foot High-Speed Tunnel. NACA RM L6H28a, 1946.

5. Loving, Donald L., and Estabrooks, Bruce B.: Transonic-Wing Investigation in the Langley 8-Foot High-Speed Tunnel at High Subsonic Mach Numbers and at A Mach Number of 1.2. Analysis of Pressure Distribution of Wing-Fuselage Configuration Having a Wing of 45° Sweepback, Aspect Ratio 4, Taper Ratio 0.6, and NACA 65A006 Airfoil Sections. NACA RM L51F07, 1951.

6. Bielat, Ralph P.: Investigation at High Speeds of a Horizontal-Tail Model in the Langley 8-Foot High-Speed Tunnel. NACA RM L6L10b, 1947.

7. Kaplan, Carl: On Similarity Rules for Transonic Flows. NACA Rep. 894, 1948. (Formerly NACA TN 1527.)

8. Kaplan, Carl: On A Solution of the Nonlinear Differential Equation for Transonic Flow past a Wave-Shaped Wall. NACA TN 2383, 1951.

9. Lindsey, W. F.: Effect of Compressibility on the Pressures and Forces Acting on a Modified NACA 65;3-019 Airfoil Having a 0.20-Chord Flap. NACA ACR L5G31a, 1946.

10. Goldstein, S., and Young, A. D.: The Linear Perturbation Theory of Compressible Flow, with Applications to Wind-Tunnel Interference. R. & M. No. 1909, British A.R.C., 1943.

11. Heaslet, Max A.: Theoretical Investigation of Methods for Computing Drag from Wake Surveys at High Subsonic Speeds. NACA ARR 5C21, 1945.

[redacted]

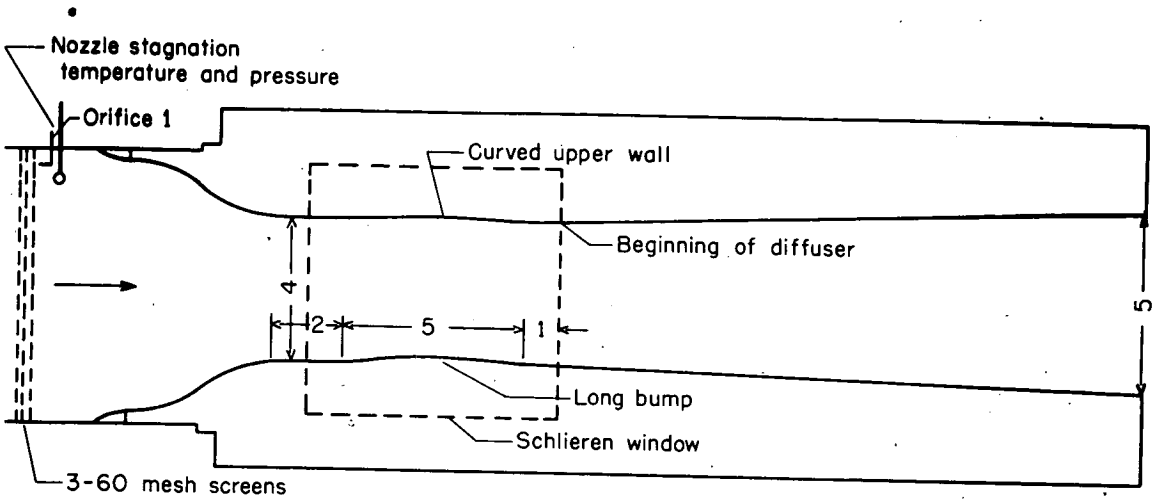

Long bump

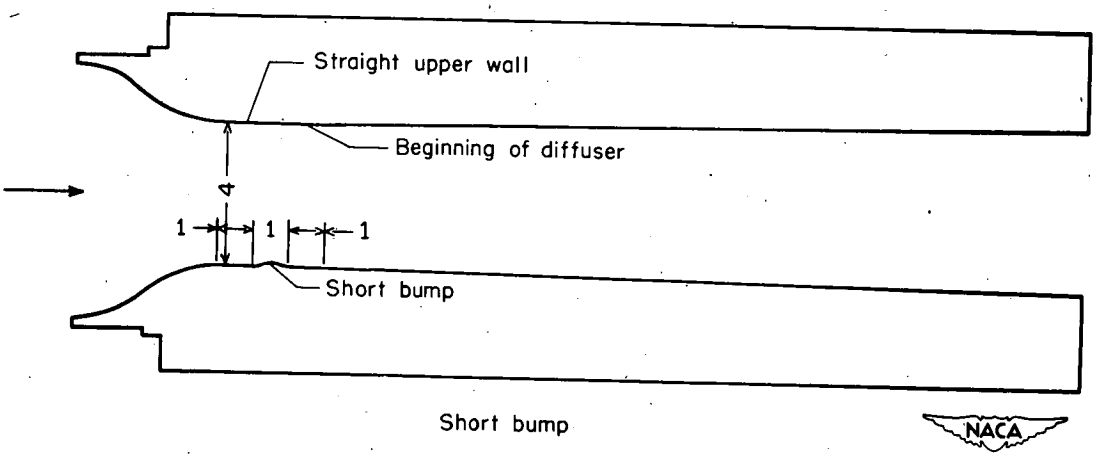

Short bump

NACA

Figure 1.- Vertical views of 1-inch-wide nozzle showing location of long and short bumps. (All dimensions in inches.)

[redacted]

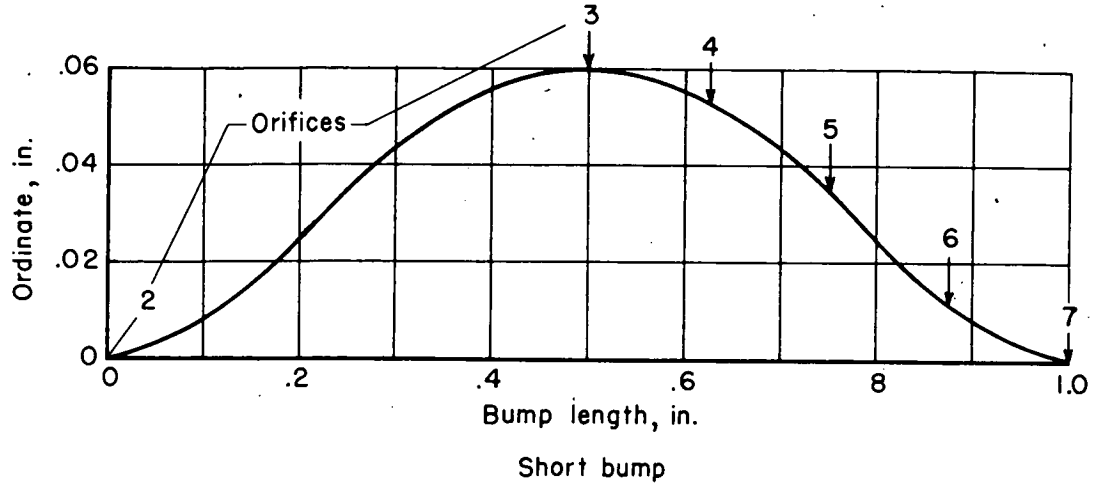

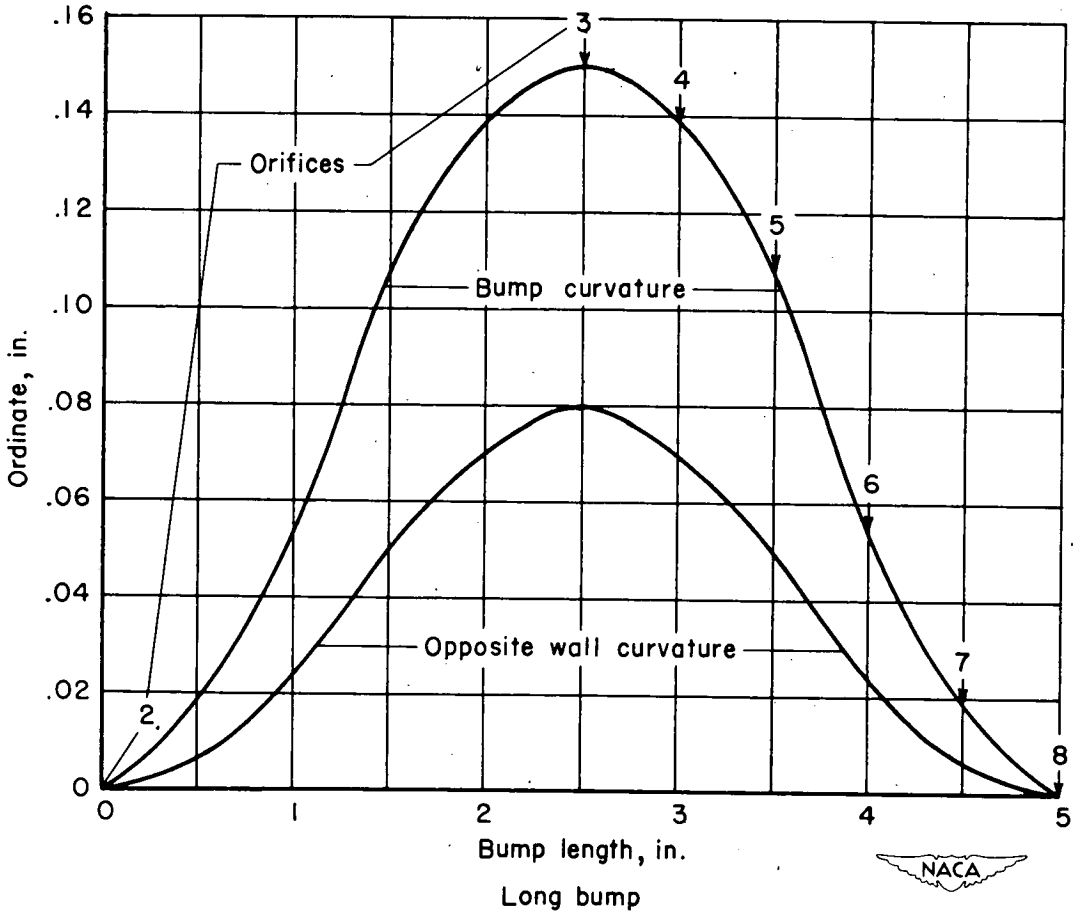

Figure 2.- Sketches of bumps showing location of orifices.

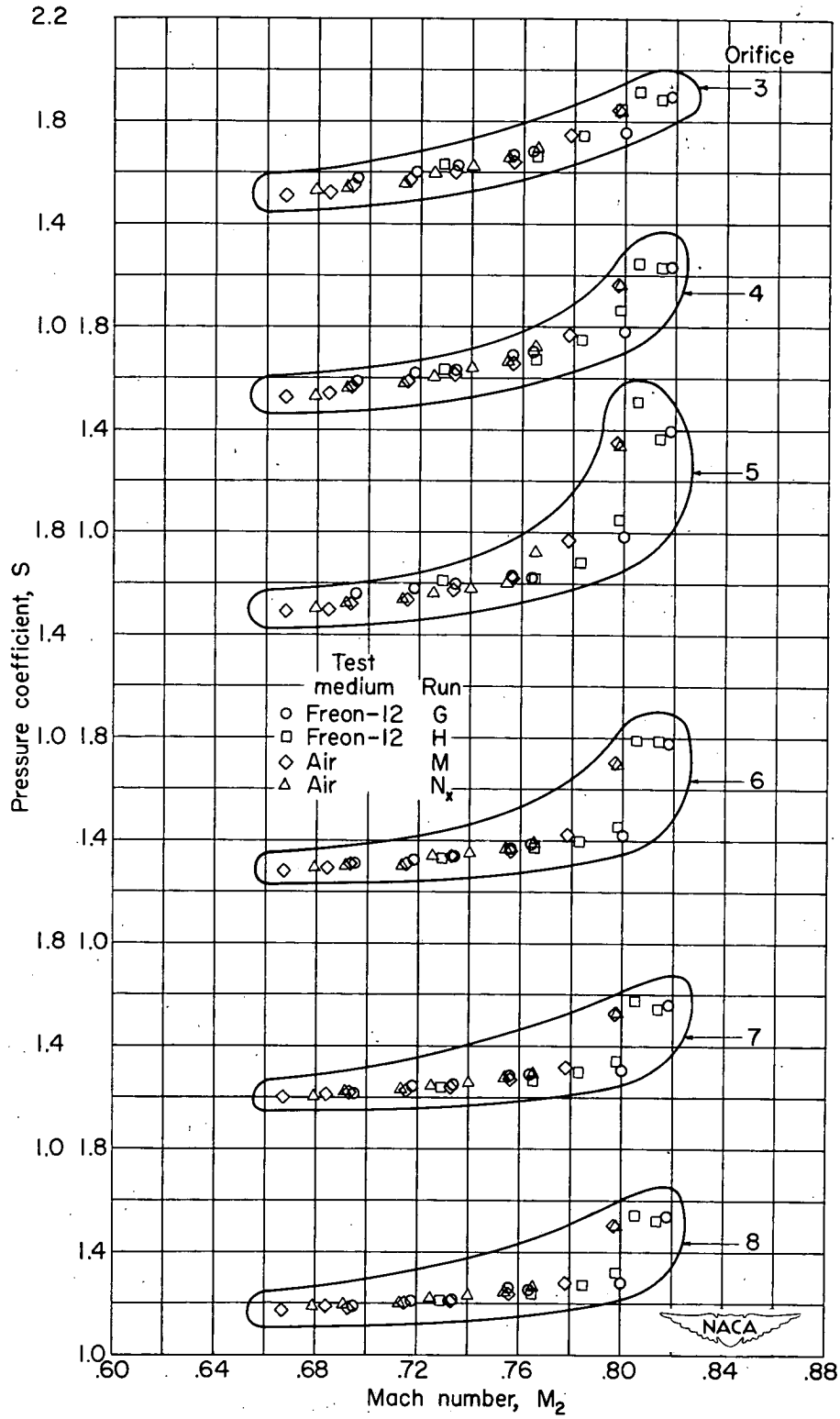

Figure 3.- Variation of pressure coefficient with M_2 at each orifice location along the long bump.

[redacted]

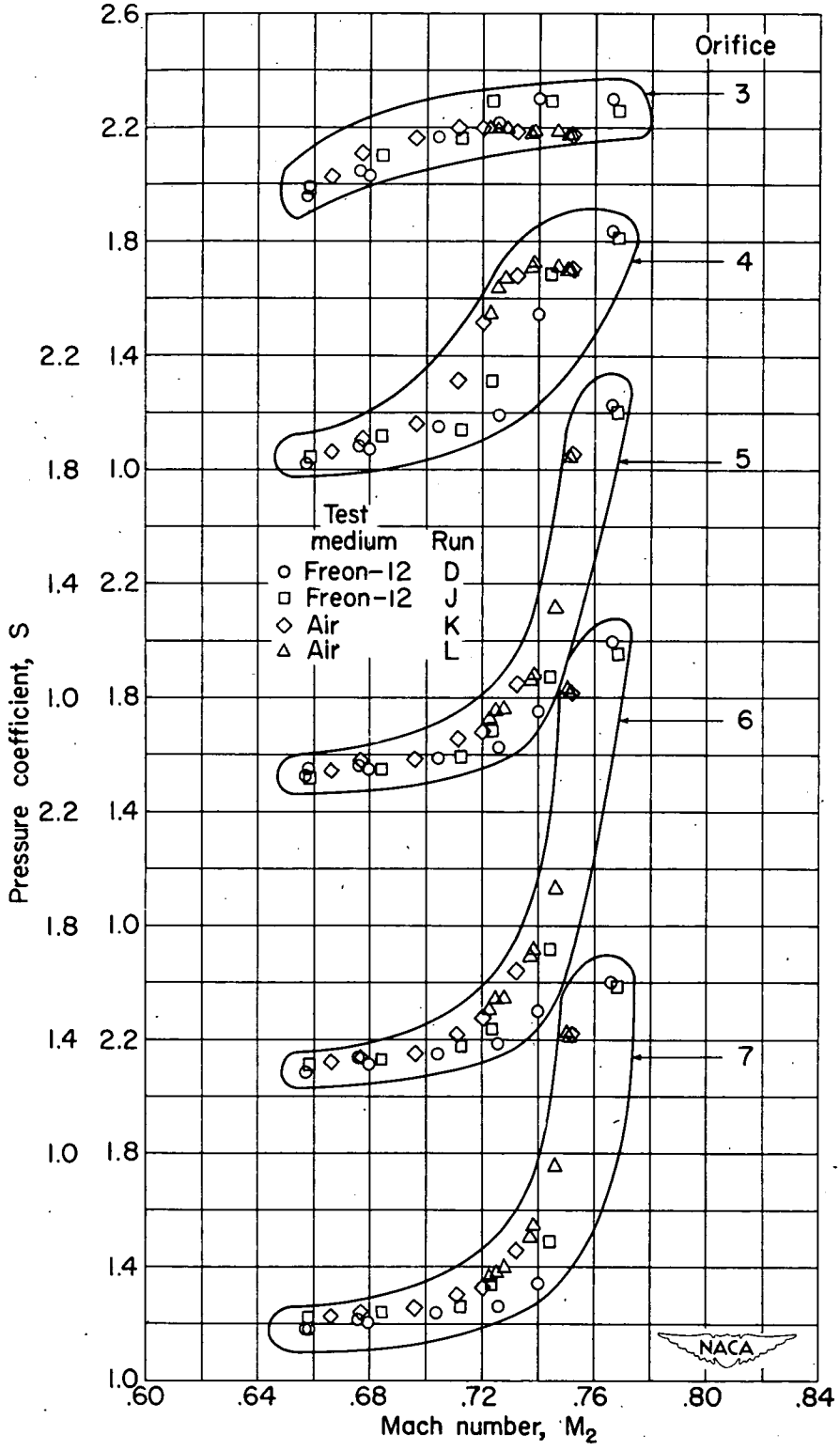

Figure 4.- Variation of pressure coefficient with M_2 at each orifice along the short bump.

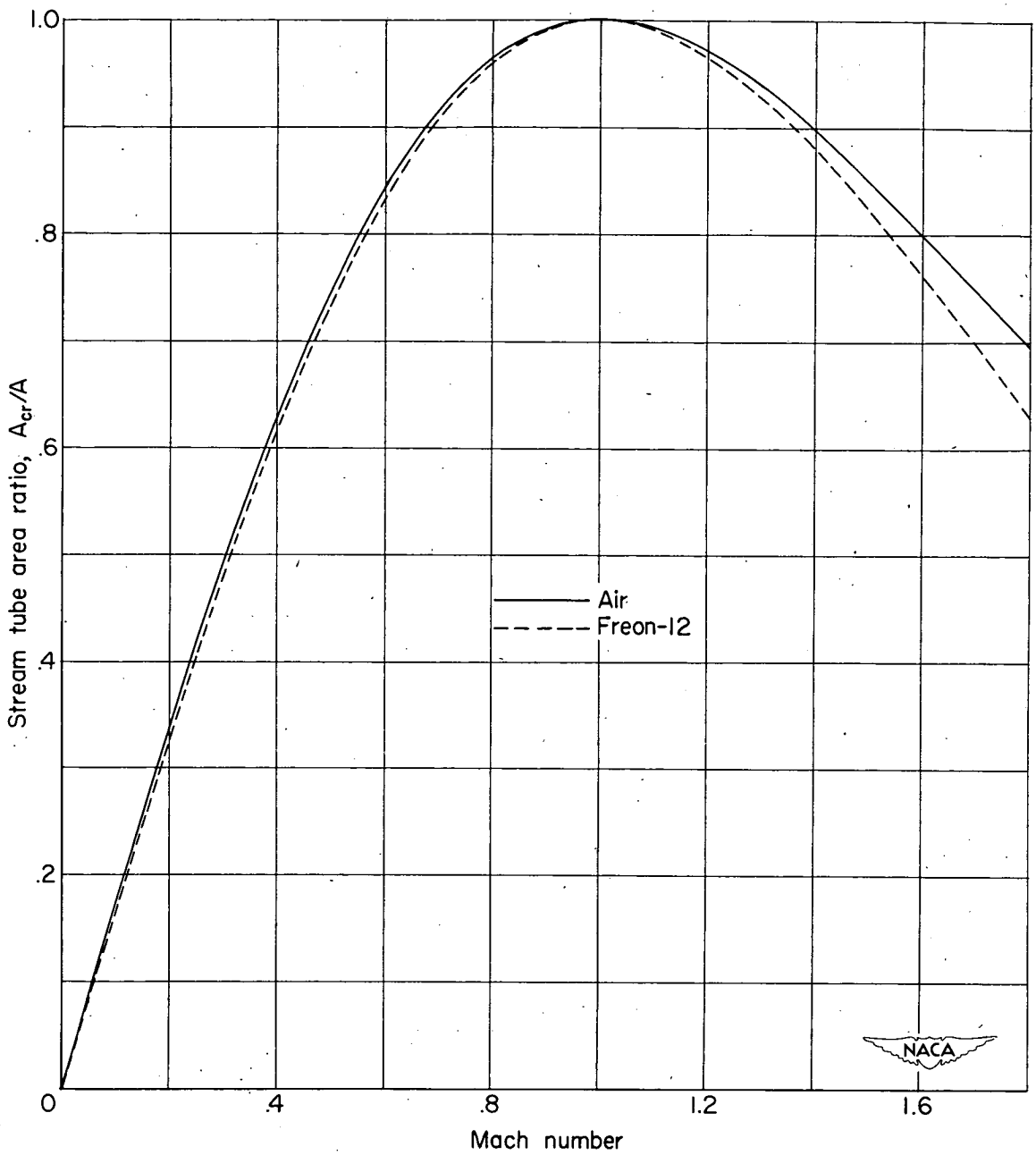

Figure 5.- Variation of stream-tube area ratio with Mach number.

[redacted]

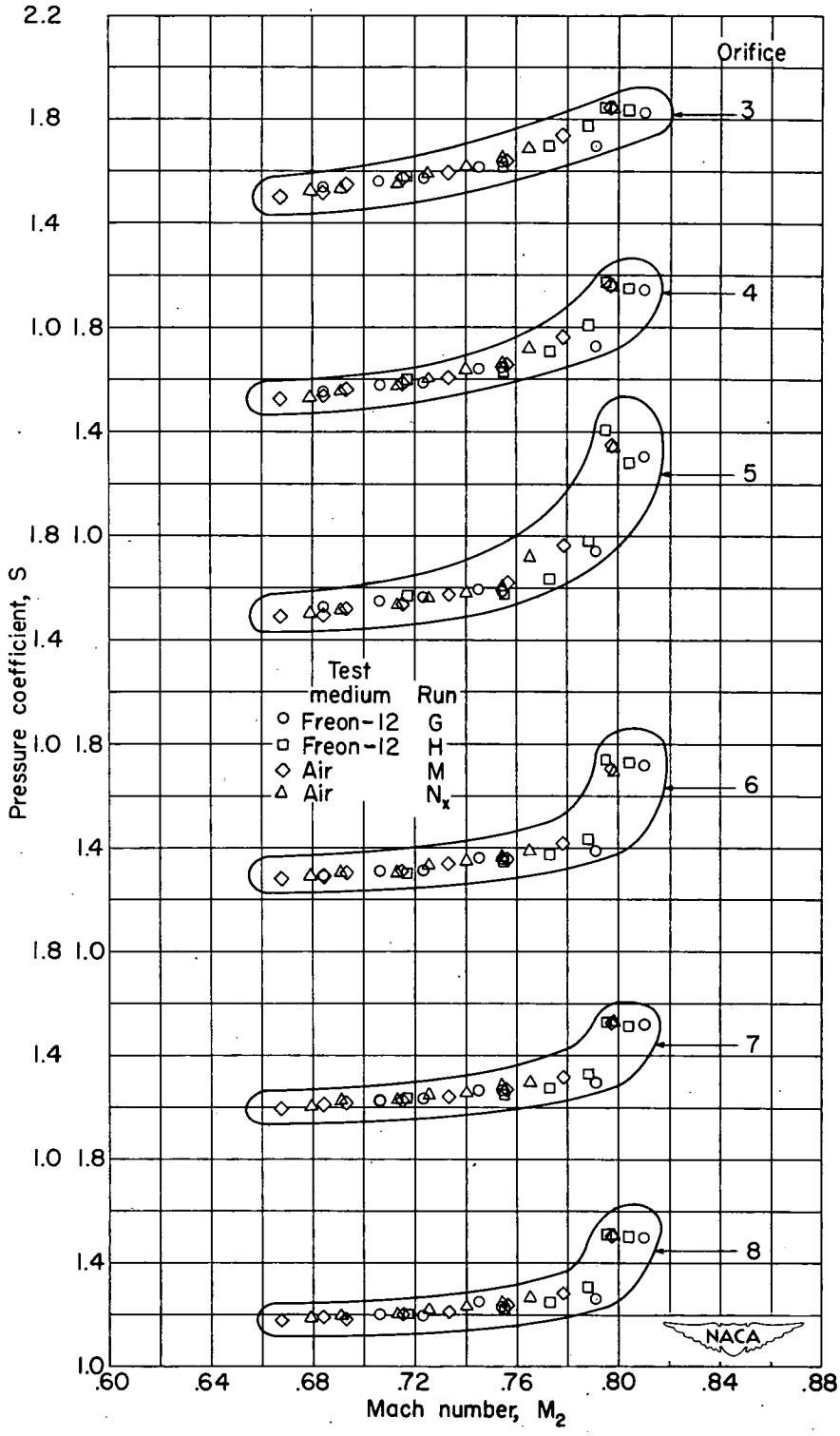

Figure 6.- Variation of pressure coefficient with M_2 at each orifice location along the long bump; Freon data converted to equivalent air values.

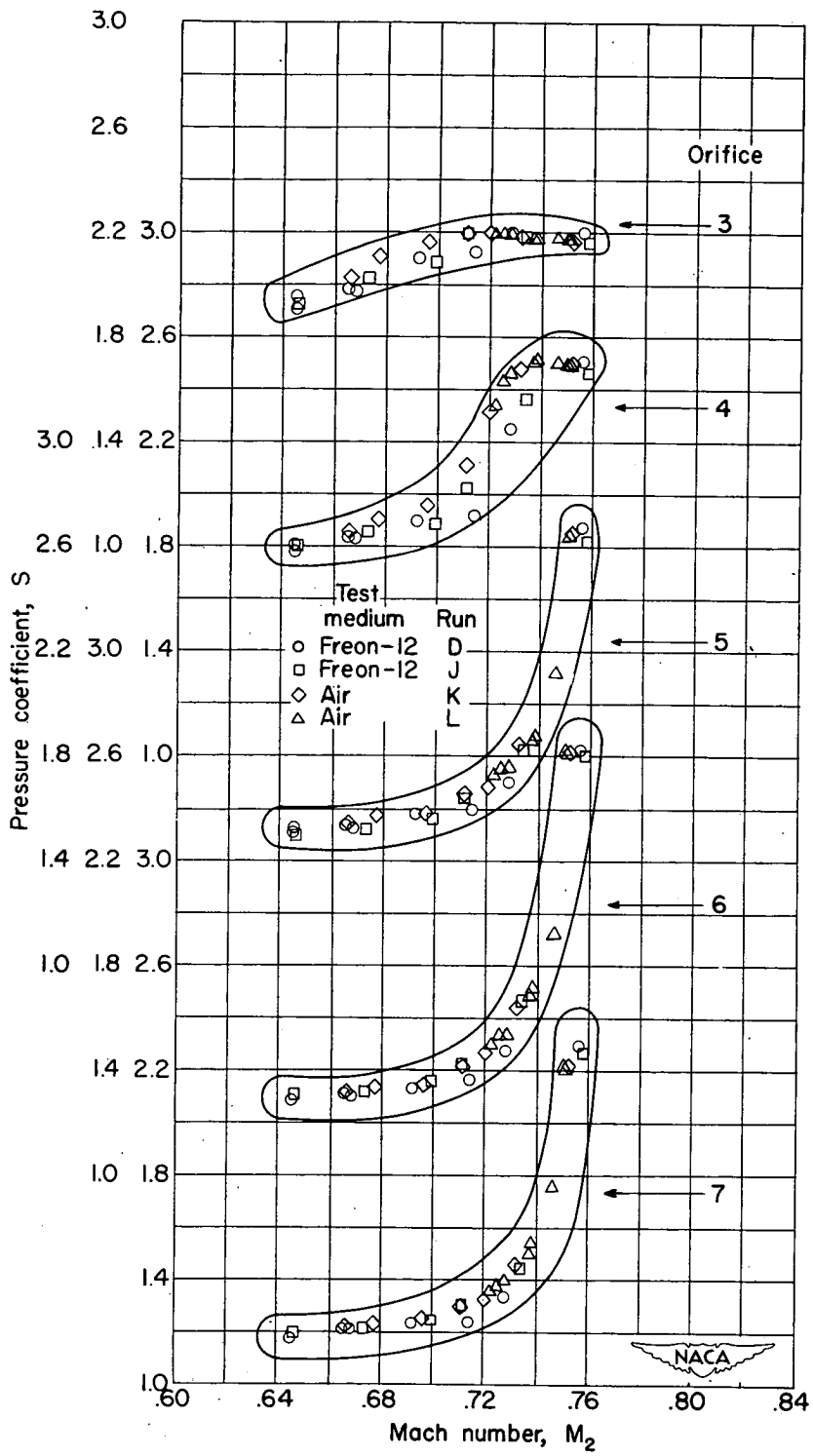

Figure 7.- Variation of pressure coefficient with M_2 at each orifice location along the short bump; Freon data converted to equivalent air values.

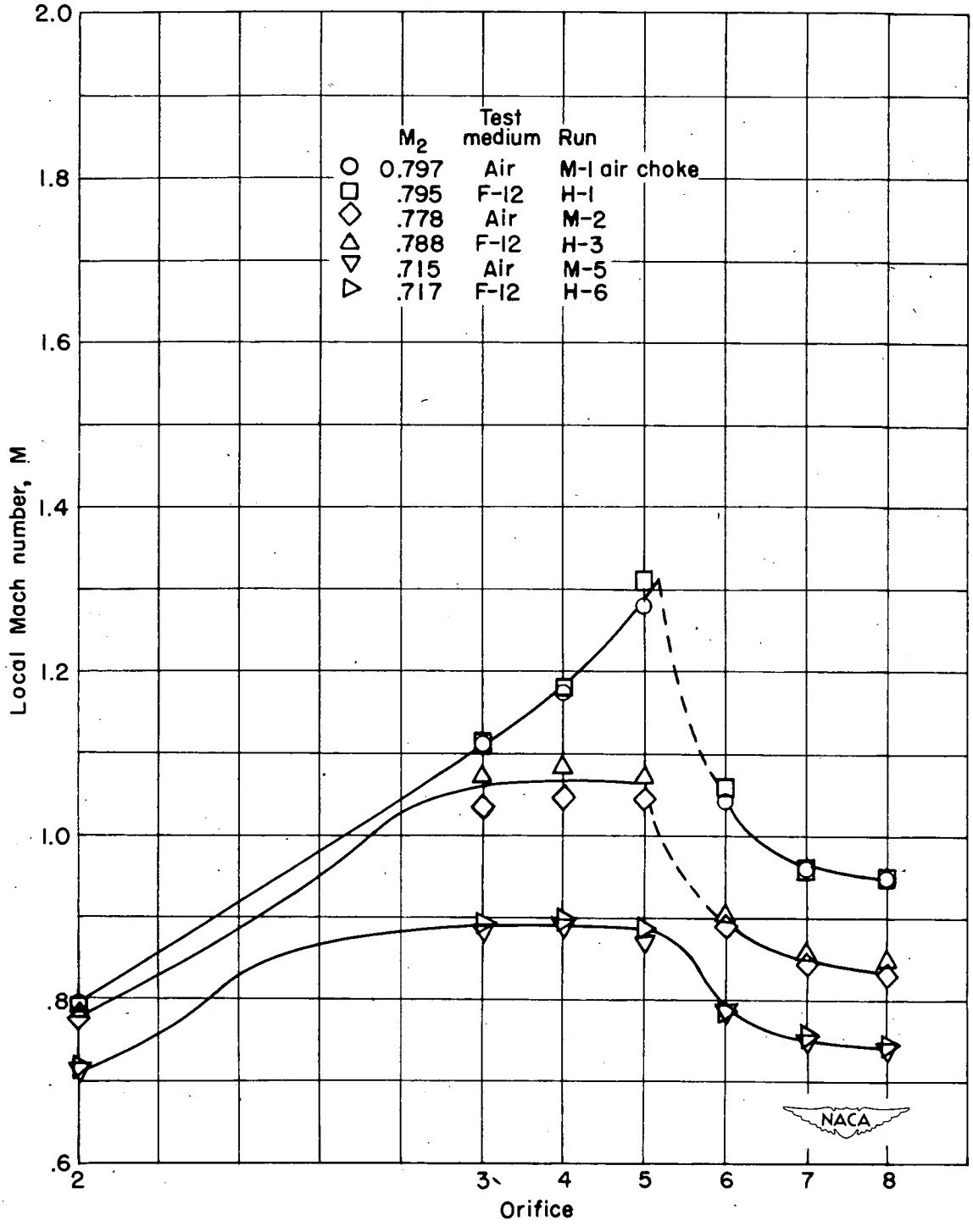

Figure 8.- Comparison of local Mach number distribution over long bump in Freon-12 and air; Freon-12 data converted to equivalent air values.

[redacted]

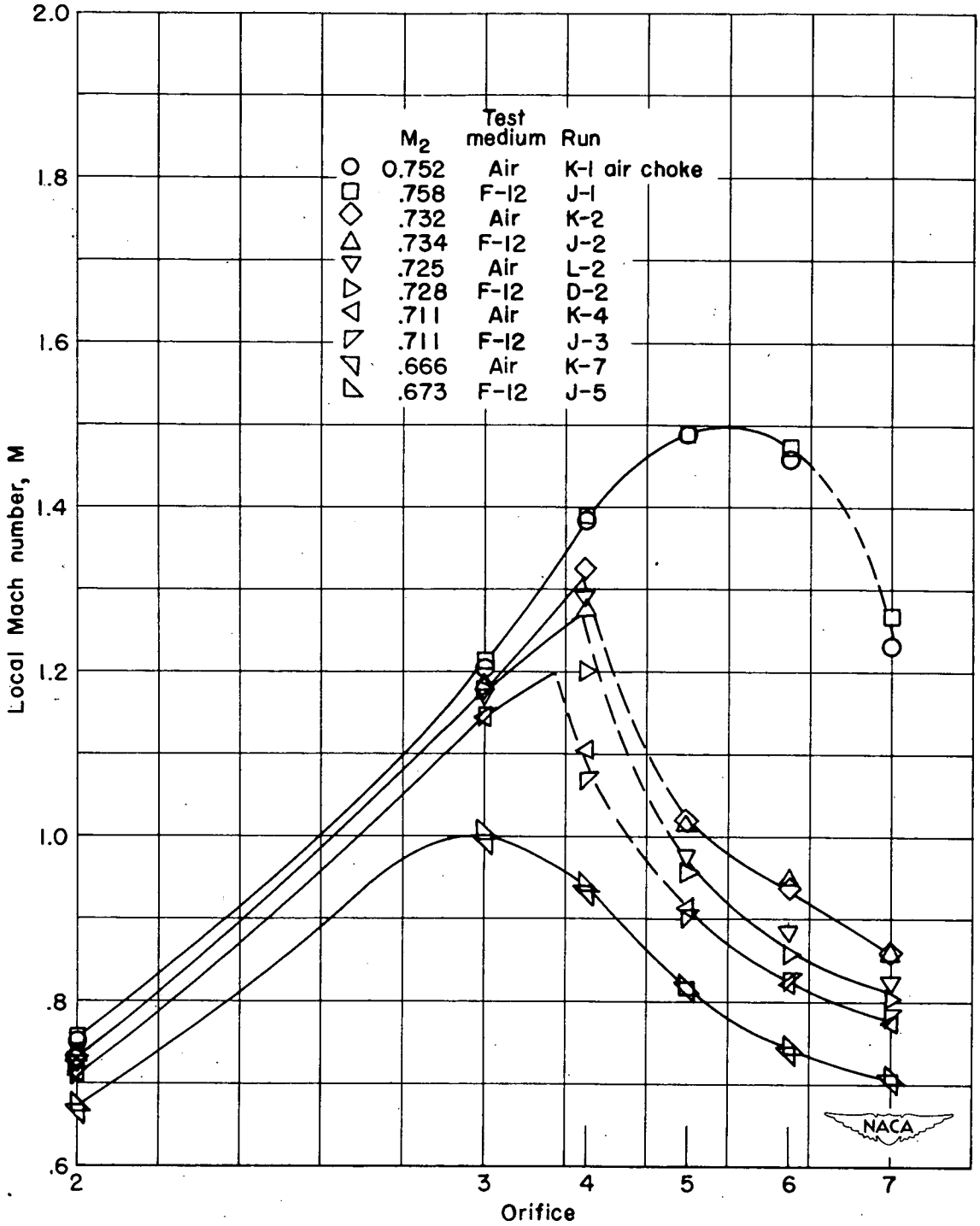

Figure 9.- Comparison of local Mach number distribution over short bump in Freon-12 and air; Freon-12 data converted to equivalent air values.

[redacted]

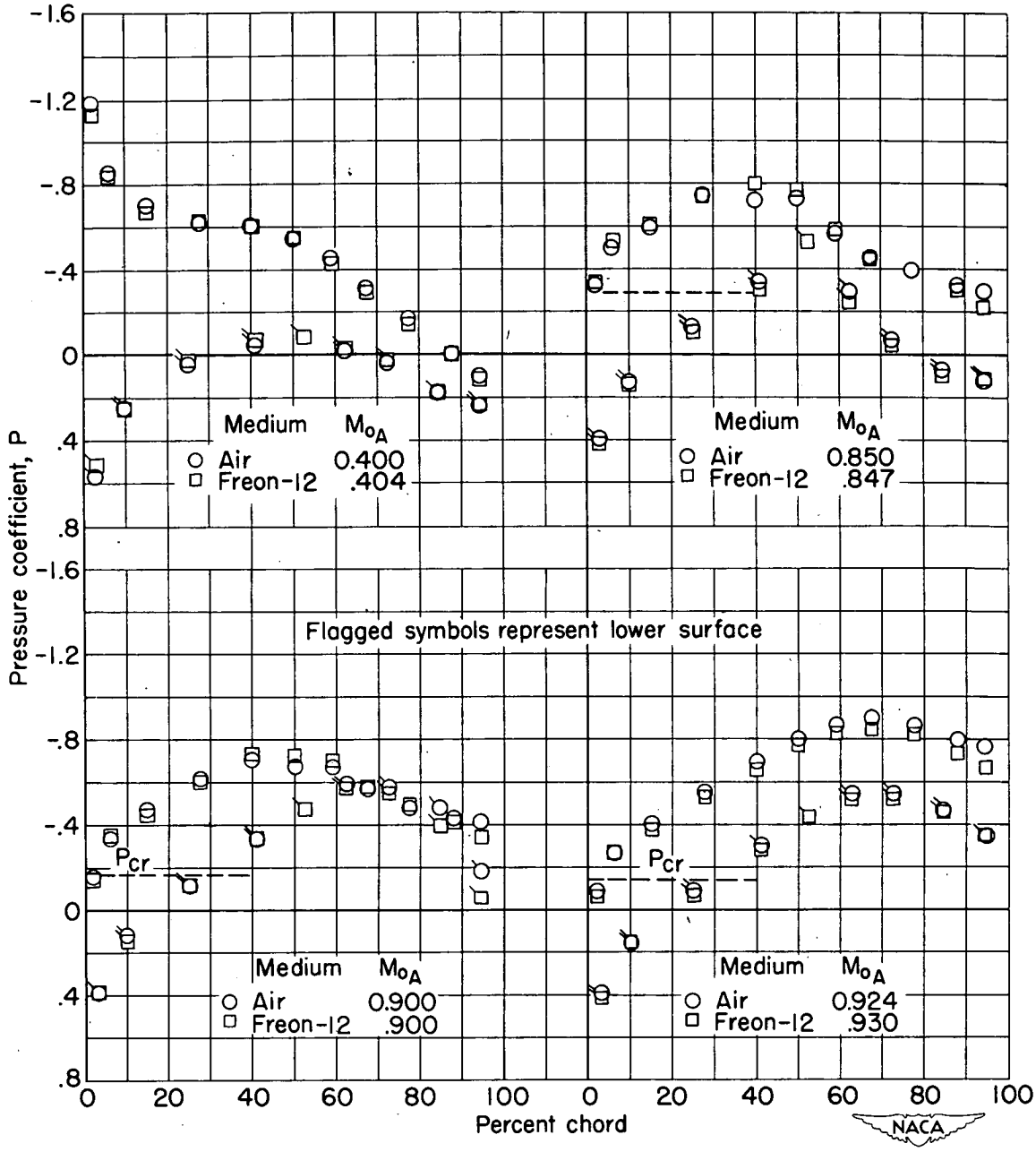

Figure 10.- Chordwise distributions of pressure at 30-percent semispan station of the NACA 65-210 wing. $\Lambda = 0^\circ$; $A = 9$; $\lambda = 0.4$; $\alpha = 4^\circ$; Freon-12 data converted to equivalent air values.

[redacted]

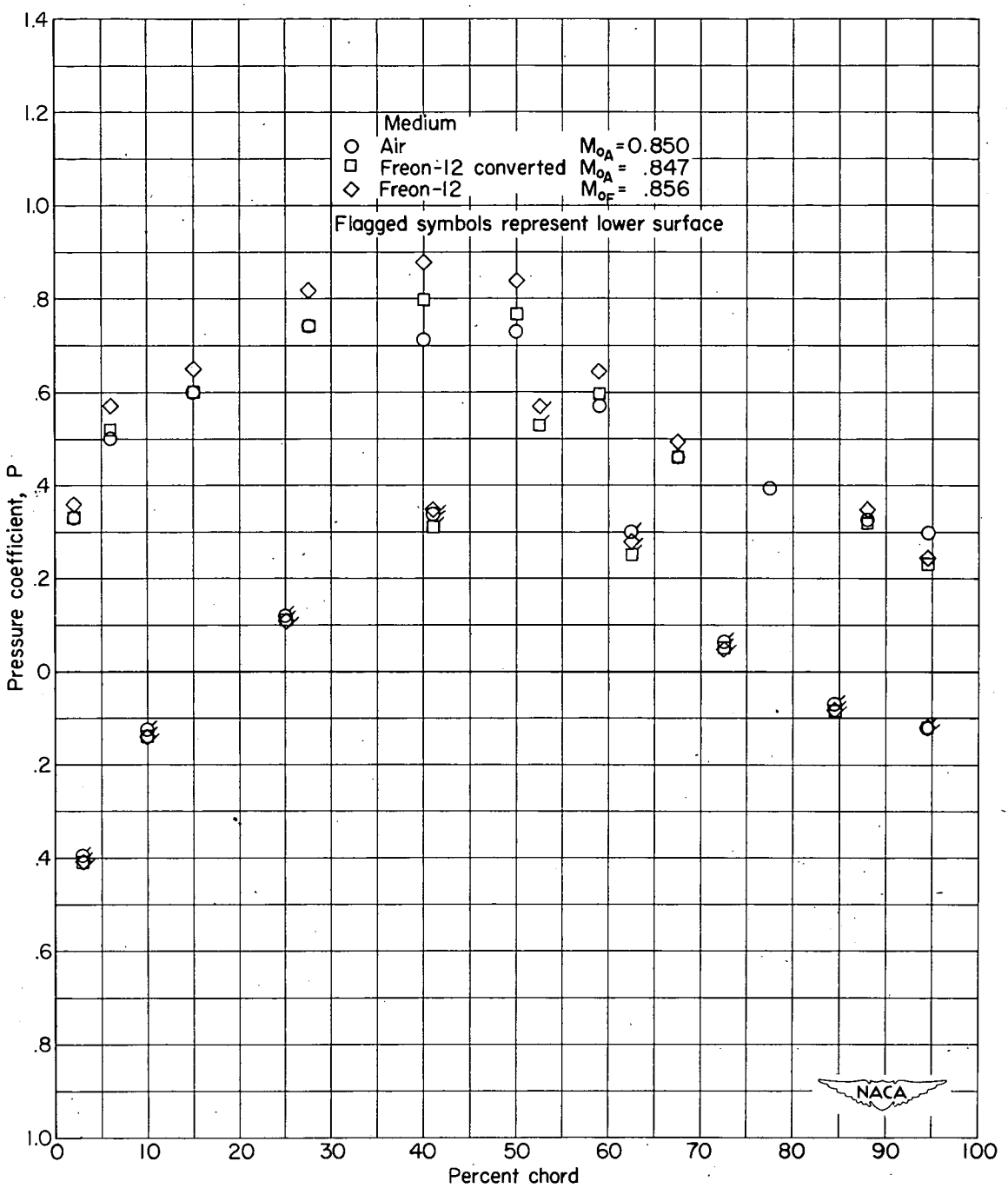

Figure 11.- Comparison of original and converted Freon pressure distributions with a corresponding pressure distribution measured in air. Configuration of figure 10.

[redacted]

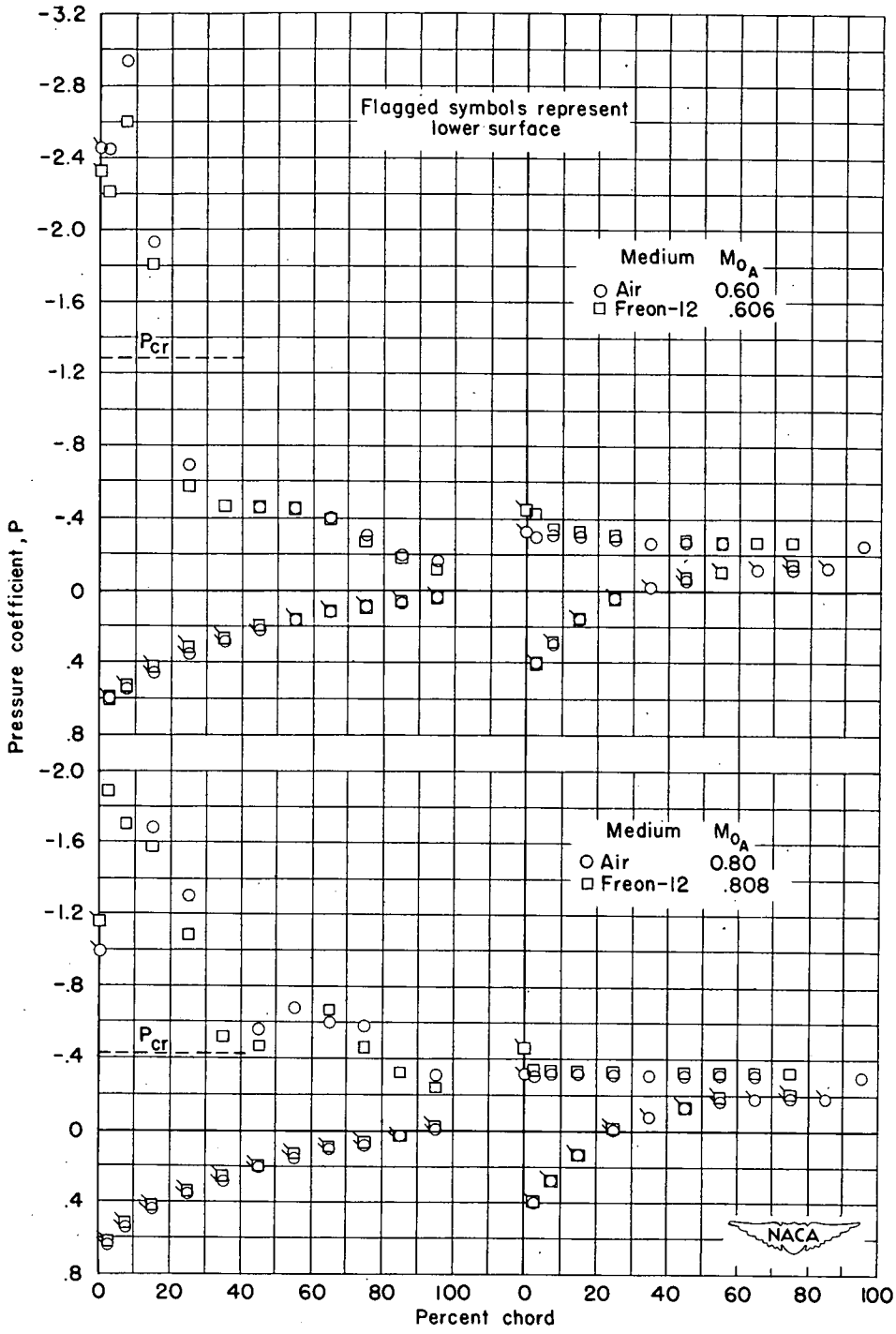

(a) Station 0.20b/2. (b) Station 0.95b/2.

Figure 12.- Chordwise distributions of pressure at two semispan stations of the NACA 65A006 wing. $\Lambda = 45^\circ$; $A = 4$; $\lambda = 0.6$; $\alpha = 14^\circ$; Freon-12 data converted to equivalent air values.

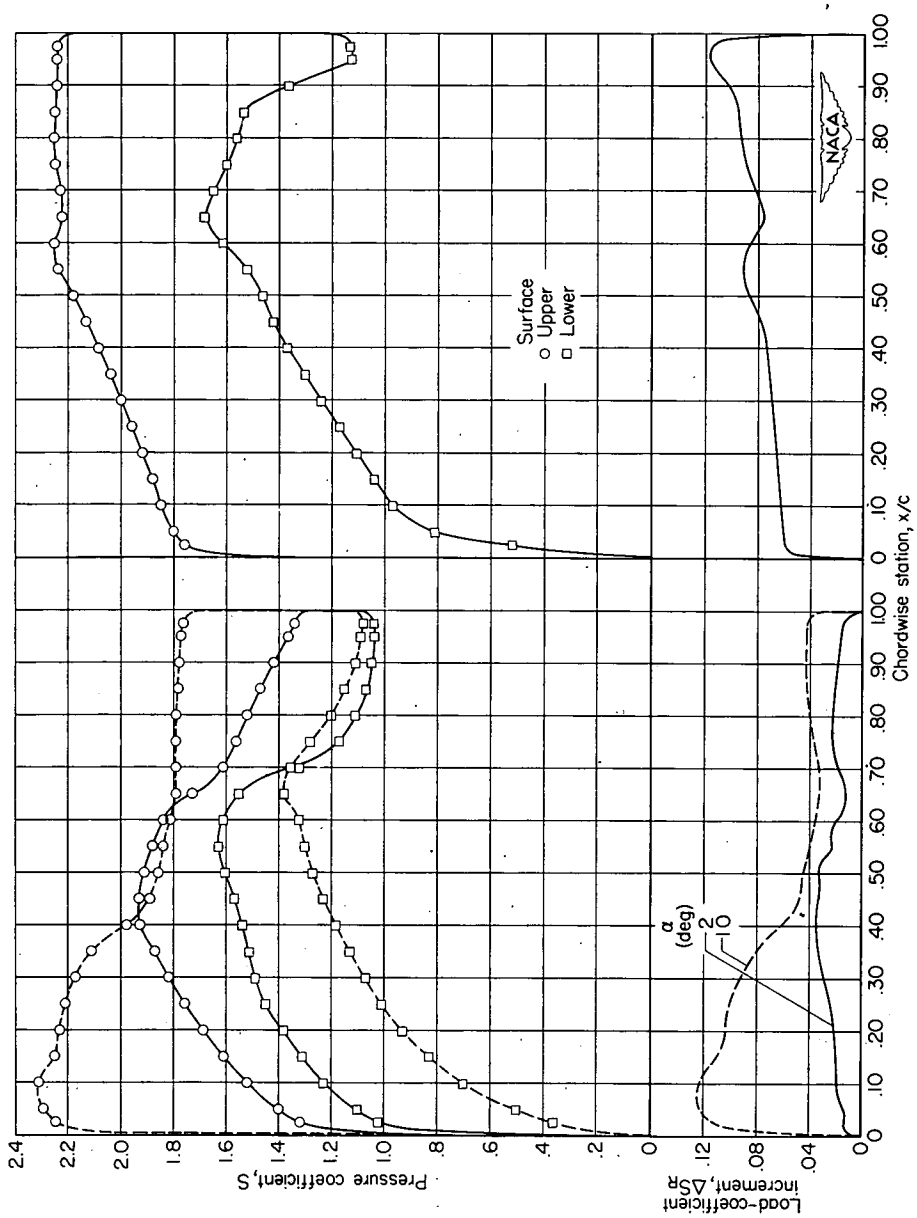

(a) M_{o_A} = 0.85 and $\alpha = 2^o$ and 10^o. (b) M_{o_A} = 0.924 and $\alpha = 7^o$.

Figure 13.- Chordwise variation of upper- and lower-surface pressure coefficients in air and the calculated load-coefficient increments required to convert from air to Freon-12 for the NACA 65-210 airfoil.

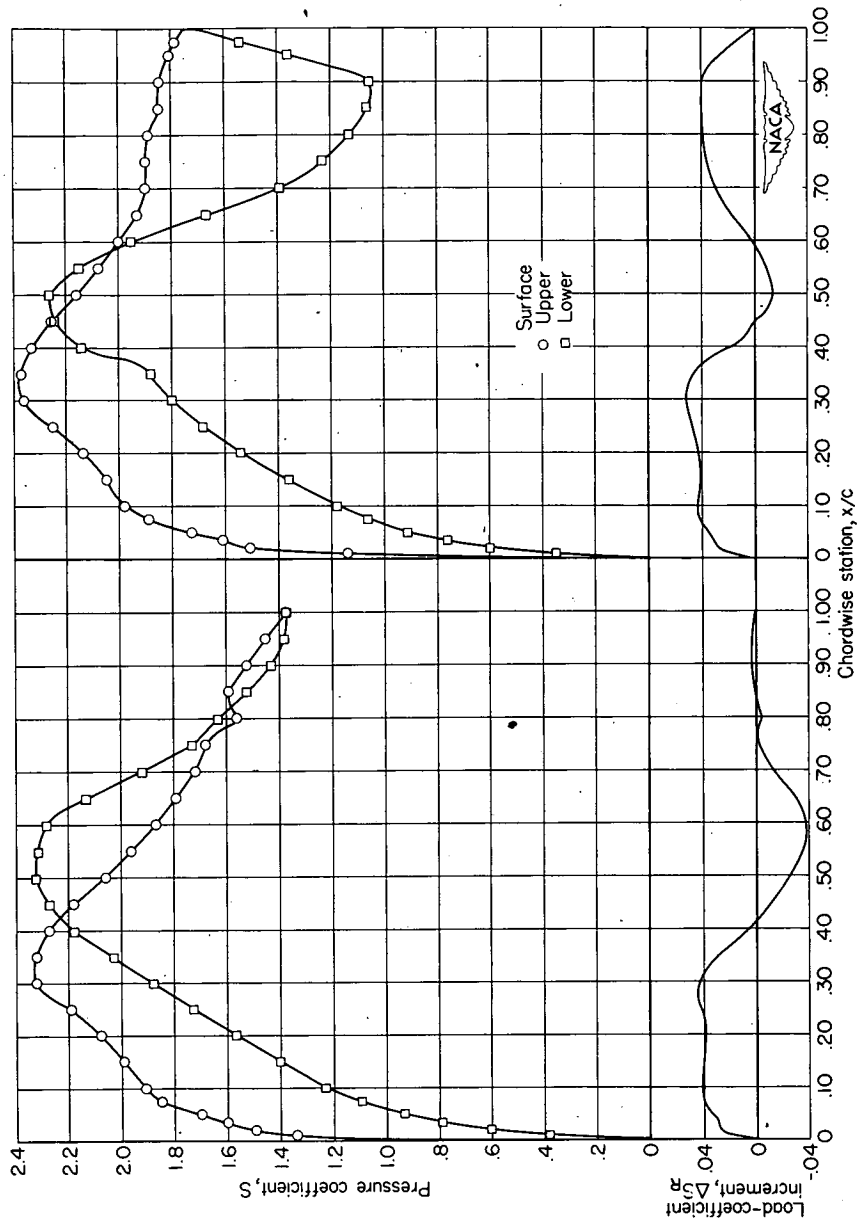

(a) $M_{O_A} = 0.729$; $\alpha = 4^\circ$, and $\delta = 0^\circ$.

(b) $M_{O_A} = 0.729$; $\alpha = 4^\circ$, and $\delta = 12^\circ$.

Figure 14.- Chordwise variation of upper- and lower-surface pressure coefficients in air and the calculated load-coefficient increments required to convert from air to Freon 12 for the NACA 65,3-019 airfoil.

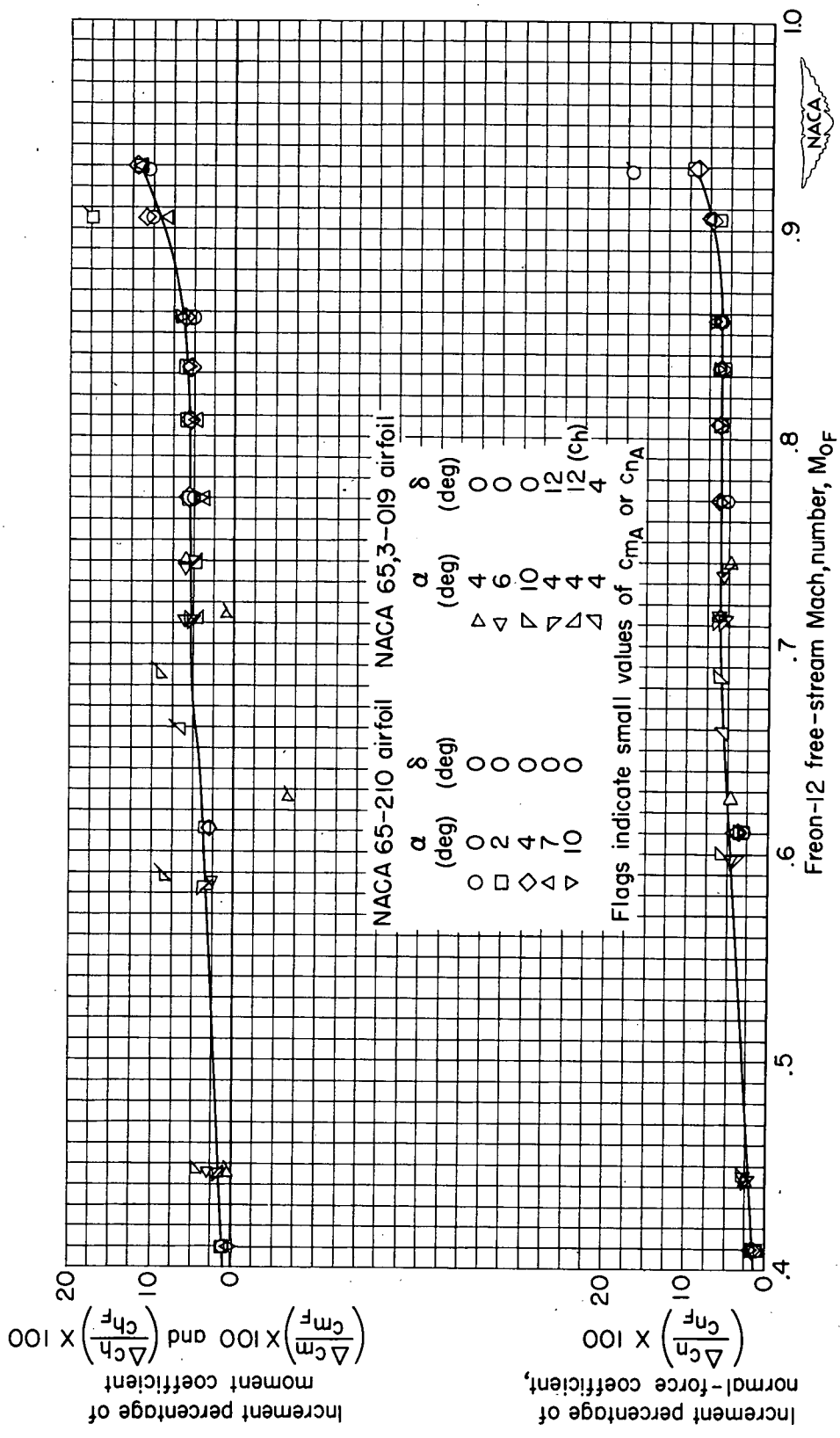

Figure 15.- Variation with Freon-12 free-stream Mach number of calculated increments required to convert lift and moment coefficients from Freon-12 to air.

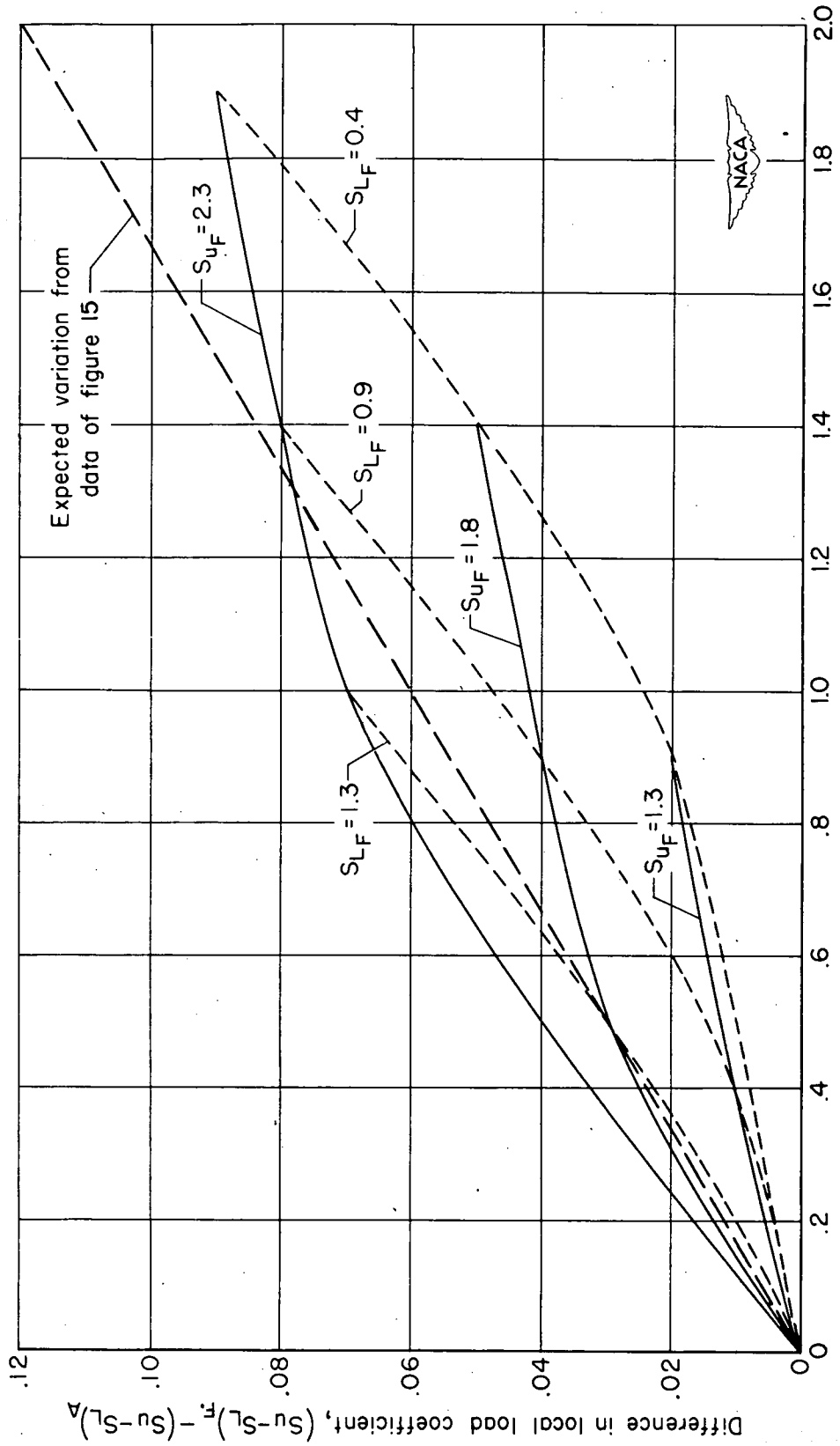

Figure 16.- Variation of difference in local load coefficient, as calculated by use of the streamline-similarity concept, with local load coefficient in Freon-12 for a free-stream Mach number of 0.80 in Freon.

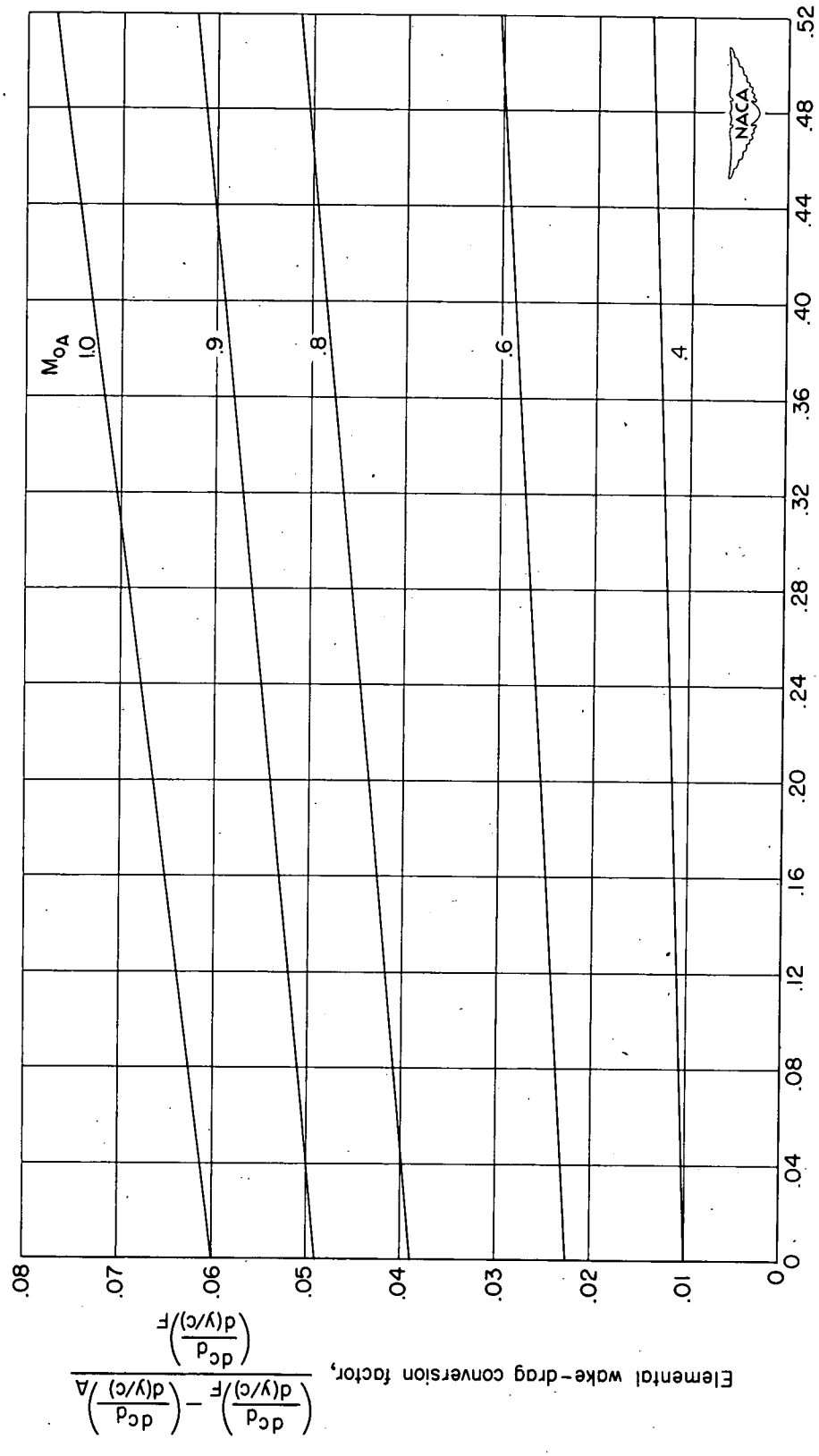

Figure 17.- Calculated variation of elemental wake-drag conversion factor with local wake total-pressure-loss coefficient in air for various free-stream Mach numbers in air.

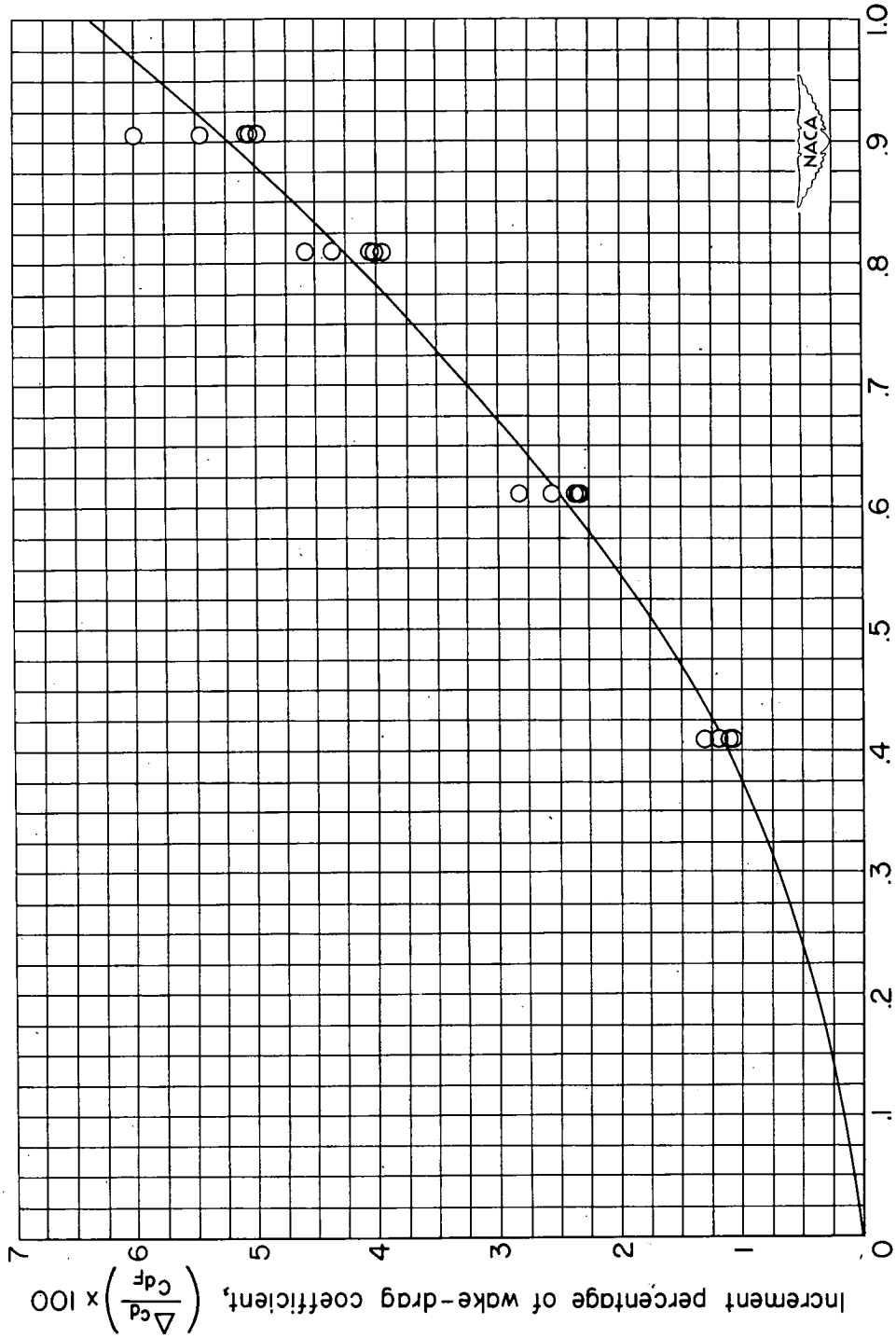

Figure 18.- Variation with Freon-12 free-stream Mach number of calculated increments required to convert wake-drag coefficient from Freon-12 to air.

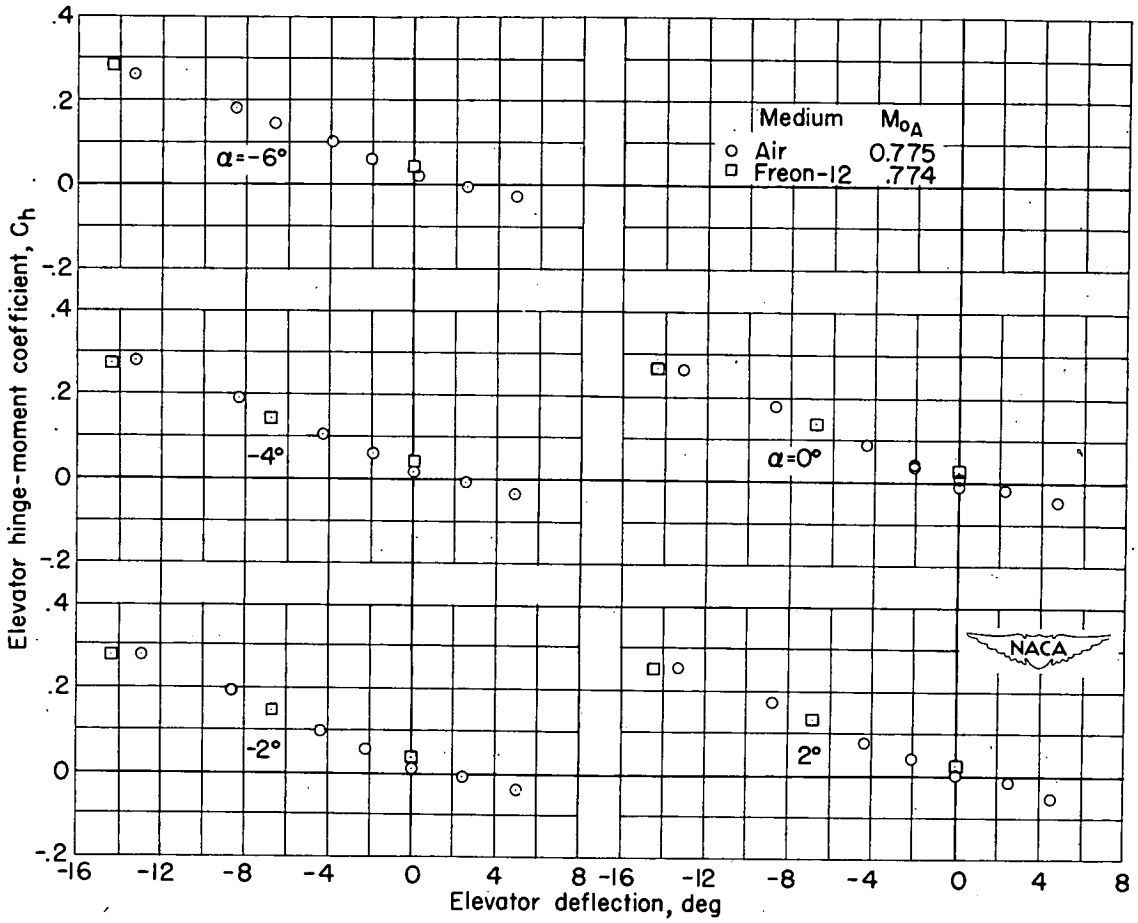

(a) $M_{o_A} \approx 0.775$.

Figure 19.- Variation of elevator hinge-moment coefficient with elevator deflection for the NACA 65-108 tail surface. $\Lambda = 0^\circ$; $A = 4.01$; $\lambda = 0.5$; Freon-12 data converted to equivalent air values.

[redacted]

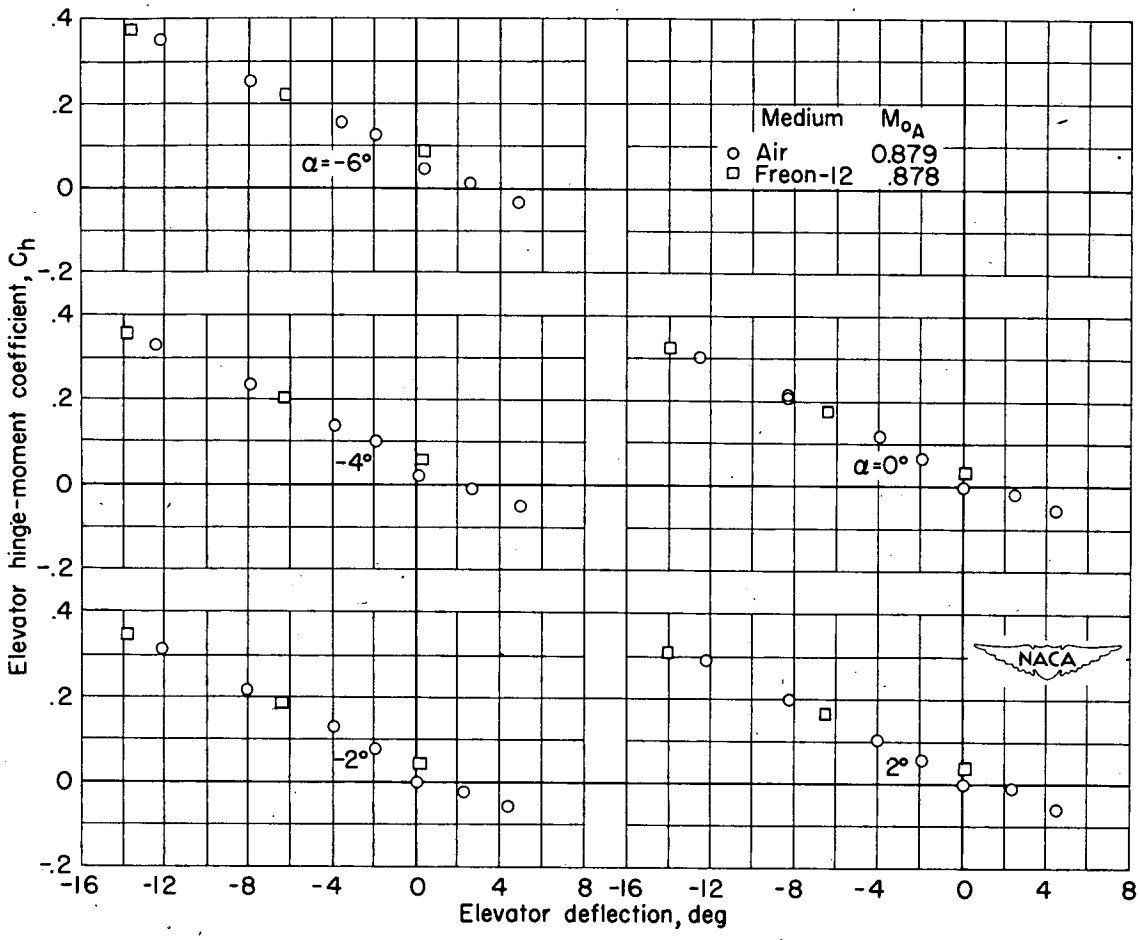

(b) $M_{o_A} \approx 0.879$.

Figure 19.- Continued.

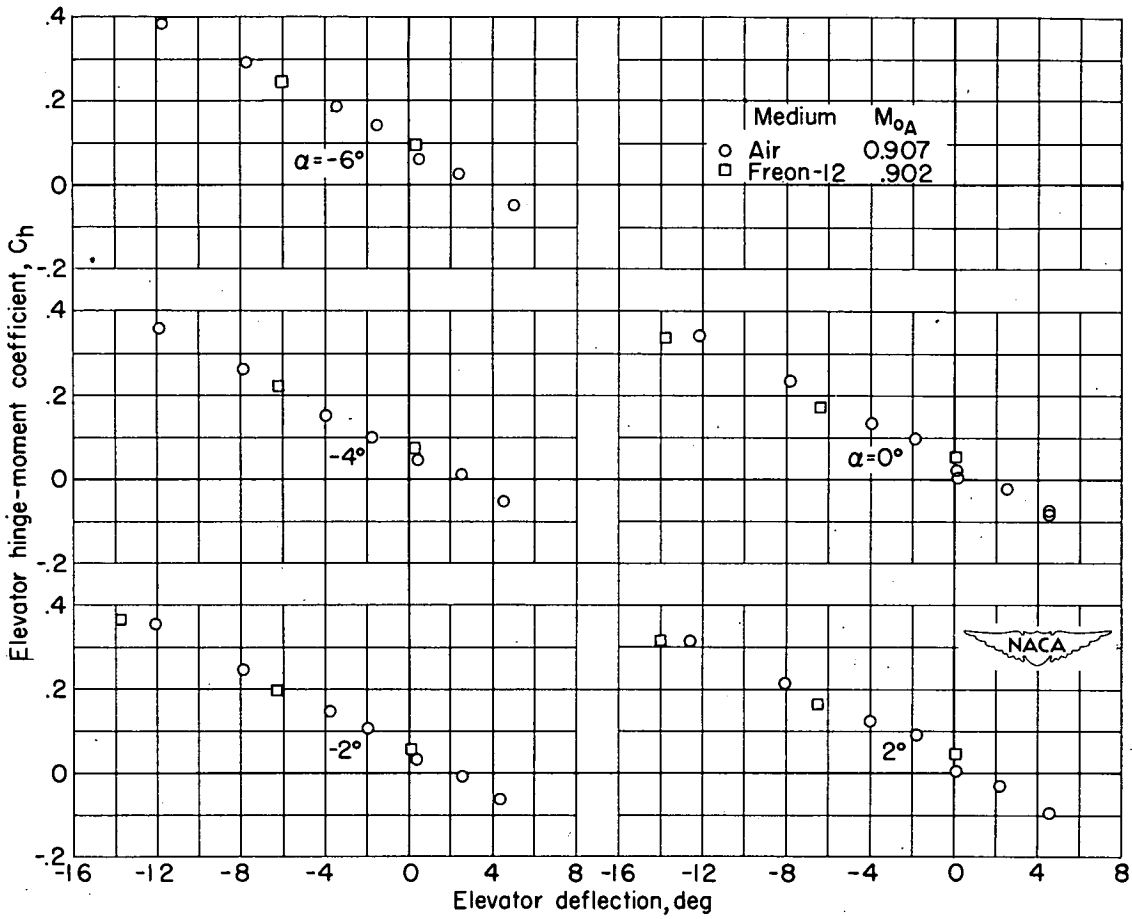

(c) $M_{o_A} \approx 0.907$.

Figure 19.- Concluded.

[redacted]

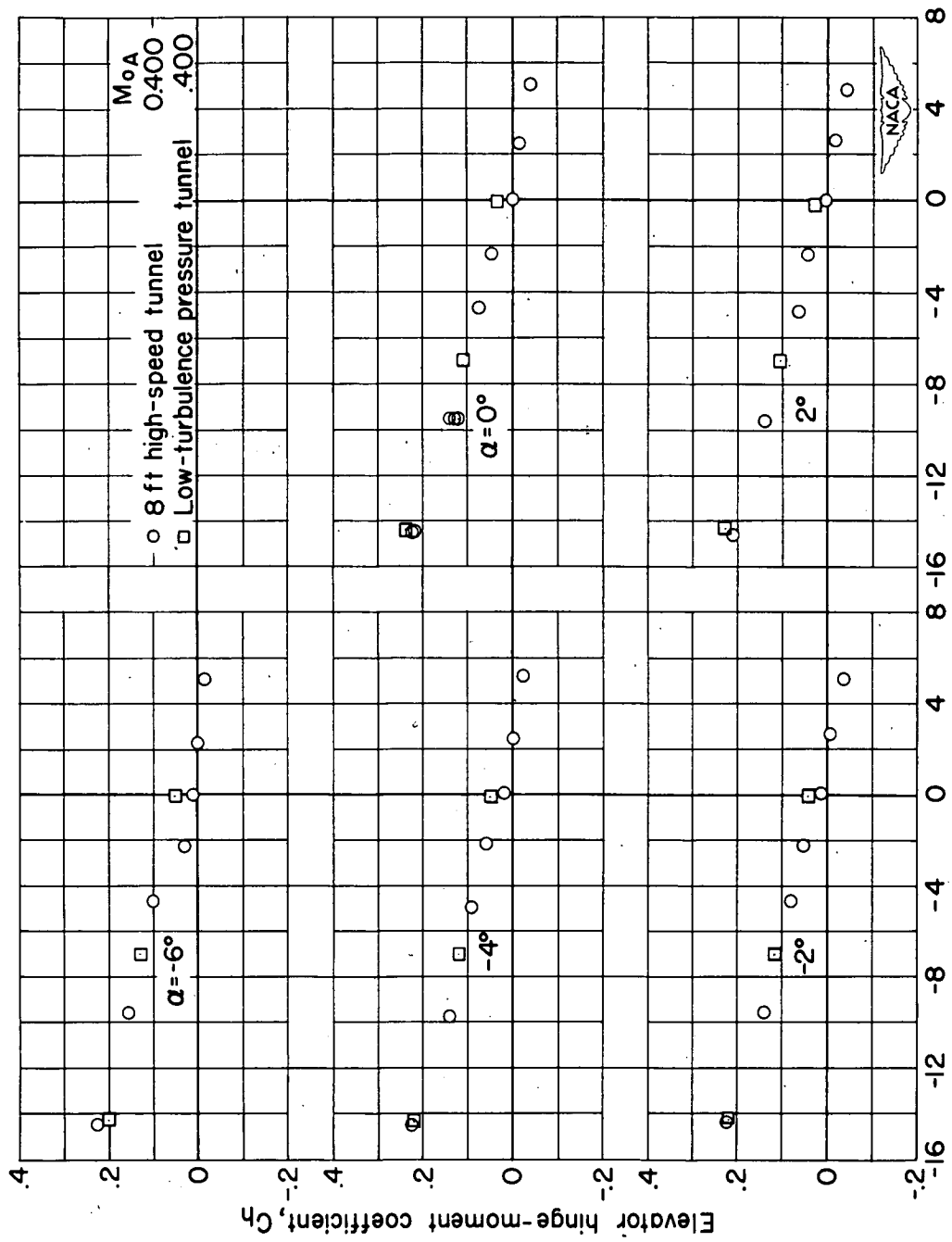

Figure 20.- Variation of elevator hinge-moment coefficient with elevator deflection as obtained only in air. Configuration of figure 19.

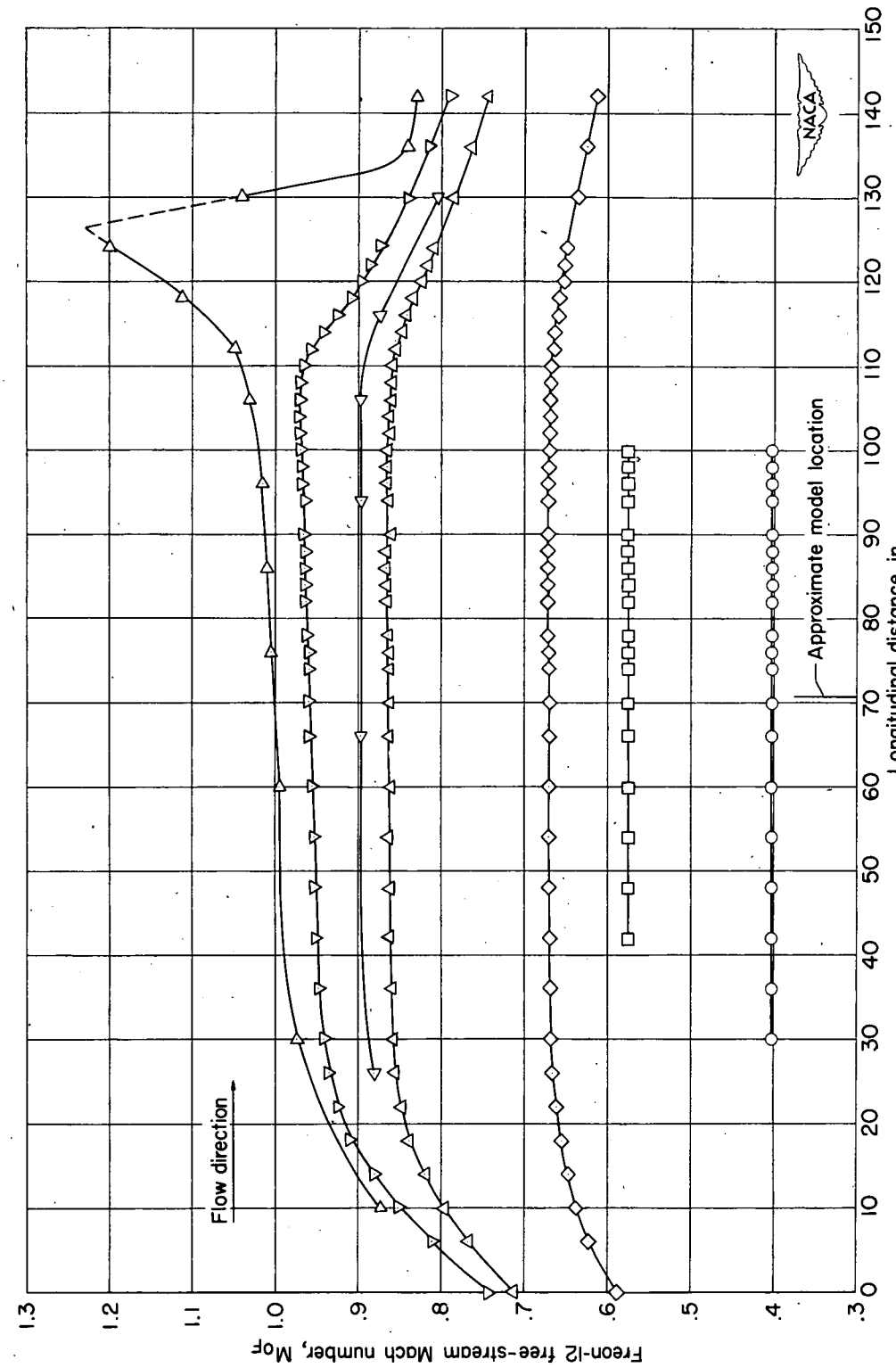

Figure 21.- Longitudinal distribution of Mach number along the center line of the Langley low-turbulence pressure tunnel with Freon-12 as a test medium.